Synthesis and the Effect of Anions on the Spectroscopy and Electrochemistry of Mono-DMSO Ligated Cobalt Corroles

Journal:	*Inorganic Chemistry*
Manuscript ID	Draft
Manuscript Type:	Article
Date Submitted by the Author:	n/a
Complete List of Authors:	Osterloh, W. Ryan; University of Houston, Chemistry Quesneau, Valentin; ICMUB, Desbois, Nicolas; Universite de Bourgogne, ICMUB Brandès, Stéphane; Universite de Bourgogne, ICMUB Shan, Wenqian; University of Houston, Chemistry Blondeau-Patissier, Virginie; Universite de Bourgogne, Temps Fréquence (ENSMM) Paolesse, Roberto; University of Rome , Science an Chemical Technology Gros, Claude; Universite de Bourgogne, LIMSAG Kadish, Karl; University of Houston, Chemistry

Synthesis and the Effect of Anions on the Spectroscopy and Electrochemistry of Mono-DMSO Ligated Cobalt Corroles

W. Ryan Osterloh,[a] Valentin Quesneau,[b] Nicolas Desbois,[b] Stéphane Brandès,[b] Wenqian Shan,[a] Virginie Blondeau-Patissier,[c] Roberto Paolesse,[*d] Claude P. Gros,[*b] Karl M. Kadish[*a]

[a]Department of Chemistry, University of Houston, Houston, TX, USA. E-mail: kkadish@uh.edu

[b]Université Bourgogne Franche-Comté, ICMUB (UMR CNRS 6302), 9 Avenue Alain Savary, BP 47870, 21078 Dijon, Cedex, France. E-mail: claude.gros@u-bourgogne.fr

[c]Department Time-Frequency, Université Bourgogne Franche-Comté, Institut FEMTO-ST (UMR CNRS 6174), 26 Chemin de l'épitaphe, 25030 Besançon Cedex, France.

[d]Department of Chemical Science and Technology, University of Rome Tor Vergata, Via della Ricerca Scientifica 1, 00133 Rome, Italy. E-mail: roberto.paolesse@uniroma2.it

ABSTRACT

A new series of cobalt A_3-triarylcorroles was synthesized and the compounds examined as to their electrochemical and spectroscopic properties in CH_2Cl_2 or DMSO containing ten different anions added to solution in the form of tetrabutylammonium salts. The investigated anions were PF_6^-, BF_4^-, HSO_4^-, ClO_4^-, Br^-, I^-, Cl^-, OAc^-, F^-, OTs^- and CN^-, all but three of which were found to facilitate reduction of the cobalt corrole in dilute CH_2Cl_2 solutions as determined by a combination of UV-visible spectroscopy and spectroelectrochemistry. The synthesized corroles are represented as $(Ar)_3CorCo(DMSO)$ where Ar is a *meso*-phenyl group containing one of 10 different electron-donating or electron-withdrawing substituents. The axial DMSO ligand was found to dissociate in dilute (10^{-5} M) CH_2Cl_2 solutions but this was not the case at the higher electrochemical concentration of 10^{-3} M where the investigated corroles exhibit a rich redox reactivity, undergoing up to five reversible one-electron transfer reactions under the different solution conditions. The reversible halfwave potentials for generation of the singly oxidized corroles varied by over 1.0 volt with change in the electron-donating or withdrawing meso-phenyl substituents and type of anion added to solution, ranging from $E_{1/2}$ = 0.83 V in one extreme to -0.42 V on the other. Much smaller shifts in potentials (on the order of ~210 mV) were observed for the reversible first reduction as a function of changing anion and/or corrole substituents, the only exception being in the case of CN^- where $E_{1/2}$ values in CH_2Cl_2 ranged from +0.08 V in solutions containing 0.1 M $TBAClO_4$ to in > -1.8 V upon addition of CN^-.

INTRODUCTION

The electrochemistry, spectroscopic characterization and coordination properties of corroles with various β-pyrrole and *meso*-substituents have been investigated under a variety of solution conditions.[1-8] These compounds have also attracted much attention over the last three decades both in terms of applications[9-16] and understanding their electronic configuration, especially the innocence or non-innocence of the macrocyclic ligand.[17-19]

Our own interest in corroles has concentrated in large part on the synthesis and characterization of new corrole derivatives with an emphasis on their spectroscopic and electrochemical properties in nonaqueous media.[8, 20-30] We have also studied the axial ligand binding reactions of corroles in their neutral, oxidized and reduced forms and recently reported how changes in coordination number influence the electrochemical and spectroscopic properties of *meso*-substituted cobalt triarylcorroles containing DMSO, CO, pyridine or NH_3 axial ligands when dissolved in a nonaqueous solvent.[31-33] The neutral cobalt corroles containing two pyridine or two NH_3 axial ligands in their formal Co(III) oxidation state generally exhibit irreversible or ill-defined reductions at relatively negative potentials, while the same compounds containing a single DMSO axial ligand are characterized by a facile and reversible one-electron transfer at relatively positive potentials.[32, 33]

Reversibility of the electron-transfer processes was seen for all of the examined mono-DMSO cobalt corroles in either CH_2Cl_2 or DMSO containing 0.1 M $TBAClO_4$ as supporting electrolyte,[32, 33] and the reduction equations were written as shown in eqs 1 and 2, where the initial redox active compound was assigned as containing a Co(II) central metal ion and a non-innocent macrocycle ligand in its cation radical form, *i.e.* $Cor^{\bullet 2-}$, as opposed to the formally trivalent anionic ligand Cor^{3-}.

$$(Ar)_3Cor^{\bullet}Co^{II}(DMSO) + e^- \rightleftharpoons [(Ar)_3CorCo^{II}]^- + DMSO \quad (1)$$

$$[(Ar)_3CorCo^{II}]^- + e^- \rightleftharpoons [(Ar)_3CorCo]^{2-} \quad (2)$$

The presence of one bound DMSO ligand on the neutral cobalt corrole and its dissociation after reduction by one electron was confirmed by a combination of electrochemical and spectroelectrochemical measurements.[32, 33] Two or three reversible one-electron oxidations were also observed for the mono-DMSO adduct with the exact potentials depending in part upon the specific *meso*-substituents of the macrocycle and in part upon the number of bound DMSO molecules on the singly oxidized form of the corrole in CH_2Cl_2 or DMSO solvent containing 0.1M $TBAClO_4$.

This current work is a continuation of our earlier studies on cobalt corroles and further explores the interacting effects of solvent, anion binding and electron-donating or withdrawing properties of the *meso*-phenyl substituents on the electrochemical and spectroscopic properties of ten newly synthesized A_3-triarylcorroles in both CH_2Cl_2 and DMSO solvents. The investigated compounds and anions utilized in this study are shown in Chart 1. An earlier study from our laboratory demonstrated a strong binding of chloride ions to the singly and doubly oxidized forms of structurally related cobalt corroles in nonaqueous media[22, 34] and a more recent manuscript from Gross and co-workers[16] showed the effect of fluoride and hydroxide ions on the catalytic activity of a pentafluorophenyl corrole Co complex (compound **1** in Chart 1) towards both oxygen reduction and water oxidation. However, there have been no systematic studies of how anions would affect not only the UV-visible spectra and redox potentials of cobalt corroles, but also their electronic configuration in nonaqueous media. This is now addressed in the current manuscript.

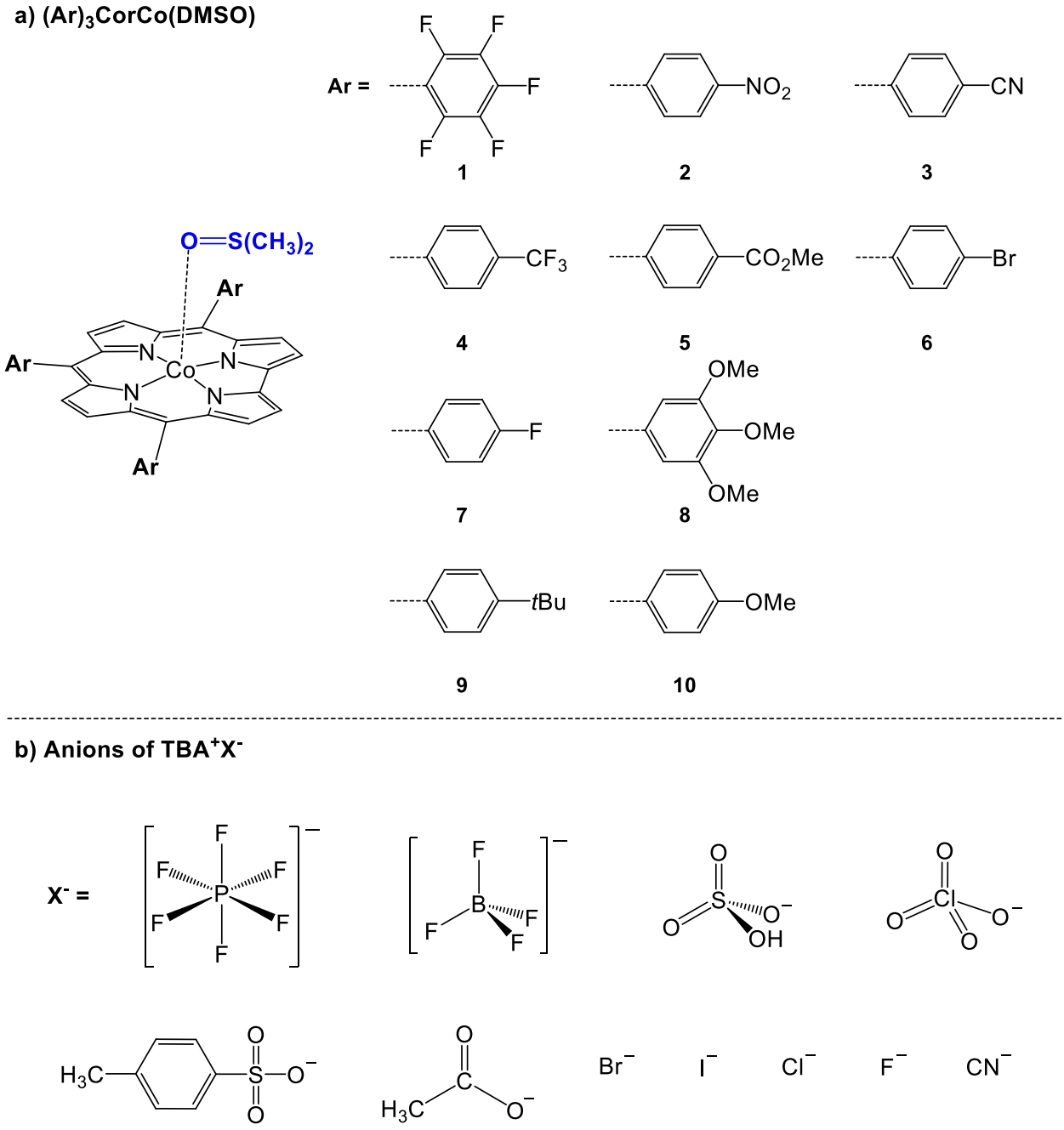

Chart 1. Structures of a) mono-DMSO ligated cobalt corroles $(Ar)_3CorCo(DMSO)$ **1**-**10** and b) added anions.

EXPERIMENTAL

Materials and Instrumentation. All chemicals and solvents were of the highest grade available and were used without further purification. Arylaldehydes were purchased from Sigma-Aldrich and pyrrole was distilled prior to use. Dichloromethane (CH_2Cl_2), methanol (MeOH) and dimethyl sulfoxide (DMSO) were purchased from Sigma Aldrich Co. and used as received. The tetra-*n*-butyl-ammonium salts (TBA^+X^-, where $X^- = PF_6^-$, BF_4^-, HSO_4^-, ClO_4^-, Br^-, I^-, Cl^-, OAc^-, F^-, OTs^-, CN^-) were purchased from Sigma Chemical Co. and used as received.

NMR solvents were purchased from Eurisotope and were used without further purification. ^1H NMR spectra were recorded on a Bruker Avance III 500 spectrometer operating at 500 MHz and available at the PACSMUB-WPCM technological platform, which relies on the “Institut de Chimie Moléculaire de l’Université de Bourgogne” and Satt Sayens "TM", a Burgundy University private subsidiary. All NMR shift values are expressed in ppm. ^1H spectra were calibrated using the residual peak of chloroform at 7.26 ppm and ^{19}F spectra were calibrated with an internal reference. To enhance resolution of the metalated corroles, ammonia or hydrazine monohydrate was added to the NMR tube

UV-visible spectra were recorded on a Hewlett-Packard Model 8453 diode array spectrophotometer. Quartz cells with optical pathlengths of 0.1 or 10 mm were used. Standard addition methods were used to determine the molar absorptivities of the new products.

MALDI-TOF mass spectra were recorded on a Bruker Ultraflex Extreme MALDI Tandem TOF Mass Spectrometer using dithranol as the matrix. ESI mass spectra were recorded on a LTQ Orbitrap XL (THERMO) instrument for HR-MS spectra.

Cyclic voltammetry was carried out at 298 K using an EG&G Princeton Applied Research 173 potentiostat/galvanostat. A three-electrode system was used for cyclic voltammetric

measurements and consisted of a glassy carbon working electrode, a platinum counter electrode and a saturated calomel reference electrode (SCE). The SCE was separated from the bulk of the solution by a fritted glass bridge of low porosity which contained the solvent/supporting electrolyte mixture. Thin-layer UV-vis spectroelectrochemical experiments were performed with a commercially available thin-layer cell from Pine Instruments Inc with a platinum honeycomb working electrode. This cell was purchased. Potentials were applied and monitored with an EG&G PAR Model 173 potentiostat. High purity N_2 from Trigas was used to deoxygenate the solution and a stream of nitrogen was kept over the solution during each electrochemical and spectroelectrochemical experiment.

Synthesis of Cobalt Corroles. In a round bottom flask, a solution of the free base corrole (0.50 mmol) and of $Co(OAc)_2 \cdot 4H_2O$ (0.60 mmol) in 60 mL of DMSO was heated and stirred at 80 °C for 40 minutes and then cooled at room temperature. The crude mixture was then poured into cold NaCl aqueous solution (around 0.8 M) and the resulting suspension was filtered and the solid was washed five times with water.

Mono-(DMSO)cobalt [5,10,15-trispentafluorophenyl]corrole, 1 was obtained as pure red powder in 97% yield starting from the free base.[35] UV-vis (CH_2Cl_2 with 1% DMSO): λ_{max}, (nm) (ε x10^{-3} L mol^{-1} cm^{-1}) 377 (72.1), 573 (12.3). ^{1}H NMR (500 MHz, $CDCl_3$+$NH_{3(g)}$), δ (ppm): 9.31 (d, $^3J_{H\text{-}H}$ = 4.2 Hz, 2H), 8.89 (d, $^3J_{H\text{-}H}$ = 4.7 Hz, 2H), 8.78-8.74 (m, 4H), 2.61 (s, 6H), -6.82 (s, 6H). ^{19}F NMR (470 MHz, $CDCl_3$+$NH_{3(g)}$) δ -137.72 (m, 6F), -154.23 (t, $^3J_{F\text{-}F}$ = 20.9 Hz, 2F), -154.48 (t, $^3J_{F\text{-}F}$ = 20.8 Hz, 1F), -162.57 (m, 4F), -162.78 (m, 2F). MS (MALDI/TOF): *m/z* 851.84 [M-DMSO]$^{+\bullet}$, 851.98 calcd for $C_{37}H_8CoF_{15}N_4$. HR-MS (ESI): m/z = 851.98236 [M-DMSO]$^{+\bullet}$, 851.98360 calcd for $C_{37}H_8CoF_{15}N_4$.

Mono-(DMSO)cobalt [5,10,15-tris(4-nitrophenyl)]corrole, 2 was obtained as pure red powder in 93% yield starting from the free base.[36] UV-vis (CH_2Cl_2 with 1% DMSO): λ_{max}, (nm) (ε x10^{-3} L mol^{-1} cm^{-1}) 377 (65.0), 580 (15.3). ^{1}H NMR (500 MHz, THF-d_8 +$NH_{3(g)}$), δ (ppm): 9.21 (d, $^3J_{H\text{-}H}$ = 4.0 Hz, 2H), 9.01 (d, $^3J_{H\text{-}H}$ = 3.5 Hz, 2H), 8.83 (d, $^3J_{H\text{-}H}$ = 4.0 Hz, 2H), 8.79 (d, $^3J_{H\text{-}H}$ = 3.5 Hz, 2H), 8.68-8.63 (m, 6H), 8.53 (d, $^3J_{H\text{-}H}$ = 7.3 Hz, 4H), 8.46 (d, $^3J_{H\text{-}H}$ = 7.3 Hz, 2H), 2.45 (s, 6H), -6.06 (s, 6H). MS (MALDI/TOF): *m/z* 716.74 $[M\text{-}DMSO]^{+\bullet}$, 717.08 calcd for $C_{37}H_{20}CoN_7O_6$. HR-MS (ESI): m/z = 717.08178 $[M\text{-}DMSO]^{+\bullet}$, 717.08016 calcd for $C_{37}H_{20}CoN_7O_6$.

Mono-(DMSO)cobalt [5,10,15-tris(4-cyanophenyl)]corrole, 3 was obtained as pure red powder in 98% yield starting from the free base.[36] UV-vis (CH_2Cl_2 with 1% DMSO): λ_{max}, (nm) (ε x10^{-3} L mol^{-1} cm^{-1}) 390 (99.2), 560 (17.9). ^{1}H NMR (500 MHz, $CDCl_3$+$NH_{3(g)}$), δ (ppm): 9.30 (d, $^3J_{H\text{-}H}$ = 4.5 Hz, 2H), 9.02 (d, $^3J_{H\text{-}H}$ = 4.5 Hz, 2H), 8.83 (d, $^3J_{H\text{-}H}$ = 4.5 Hz, 4H), 8.44 (d, $^3J_{H\text{-}H}$ = 7.8 Hz, 4H), 8.37 (d, $^3J_{H\text{-}H}$ = 7.8 Hz, 2H), 8.10-8.06 (m, 6H), 2.61 (s, 6H), -6.74 (s, 6H). MS (MALDI/TOF): *m/z* 656.71 $[M\text{-}DMSO]^{+\bullet}$, 657.12 calcd for $C_{40}H_{20}CoN_7$. HR-MS (ESI): m/z = 657.11110 $[M\text{-}DMSO]^{+\bullet}$, 657.11067 calcd for $C_{40}H_{20}CoN_7$.

Mono-(DMSO)cobalt [5,10,15-tris(4-trifluoromethylphenyl)]corrole, 4 was obtained as pure red powder in 83% yield starting from the free base.[36] UV-vis (CH_2Cl_2 with 1% DMSO): λ_{max}, (nm) (ε x10^{-3} L mol^{-1} cm^{-1}) 384 (72.6), 566 (13.7). ^{1}H NMR (500 MHz, $CDCl_3$+$NH_{3(g)}$), δ (ppm): 9.28 (d, $^3J_{H\text{-}H}$ = 4.3 Hz, 2H), 9.03 (d, $^3J_{H\text{-}H}$ = 4.3 Hz, 2H), 8.83 (d, $^3J_{H\text{-}H}$ = 4.3 Hz, 4H), 8.45 (d, $^3J_{H\text{-}H}$ = 7.8 Hz, 4H), 8.37 (d, $^3J_{H\text{-}H}$ = 7.8 Hz, 2H), 8.06 (d, $^3J_{H\text{-}H}$ = 7.8 Hz, 2H), 8.03 (d, $^3J_{H\text{-}H}$ = 7.8 Hz, 2H), 8.07-8.02 (m, 6H), 2.61 (s, 6H), -6.74 (s, 6H). ^{19}F NMR (470 MHz, $CDCl_3$+$NH_{3(g)}$) δ -61.81(s, 3F), -61.84 (s, 6F). MS (MALDI/TOF): *m/z* 785.88 $[M\text{-}DMSO]^{+\bullet}$, 786.09 calcd for $C_{40}H_{20}CoF_9N_4$. HR-MS (ESI): m/z = 786.08652 $[M\text{-}DMSO]^{+\bullet}$, 786.08708 calcd for $C_{40}H_{20}CoF_9N_4$.

Mono-(DMSO)cobalt [5,10,15-tris(4-carboxymethylphenyl)]corrole, 5 was obtained as pure red powder in 86% yield starting from the free base.[36] UV-vis (CH_2Cl_2 with 1% DMSO): λ_{max}, (nm) (ε x10^{-3} L mol^{-1} cm^{-1}) 390 (83.5), 570 (15.2). ^{1}H NMR (500 MHz, CDCl3+$NH_{3(g)}$), δ (ppm): 9.26 (d, $^3J_{H\text{-}H}$ = 4.2 Hz, 2H), 9.05 (d, $^3J_{H\text{-}H}$ = 4.7 Hz, 2H), 8.87-8.84 (m, 4H), 8.49-8.39 (m, 10H), 8.34 (d, $^3J_{H\text{-}H}$ = 7.8 Hz, 2H), 4.10 (s, 9H), 2.61 (s, 6H), -6.75 (s, 6H). MS (MALDI/TOF): *m/z* 755.95 $[M\text{-}DMSO]^{+\bullet}$, 756.15 calcd for $C_{43}H_{29}CoN_4O_6$. HR-MS (ESI): m/z = 756.14221 $[M\text{-}DMSO]^{+\bullet}$, 756.14136 calcd for $C_{43}H_{29}CoN_4O_6$.

Mono-(DMSO)cobalt [5,10,15-tris(4-bromophenyl)]corrole, 6 was obtained as pure red powder in 92% yield starting from the free base.[36] UV-vis (CH_2Cl_2 with 1% DMSO): λ_{max}, (nm) (ε x10^{-3} L mol^{-1} cm^{-1}) 390 (94.6), 566 (16.2). ^{1}H NMR (500 MHz, $CDCl_3$+$NH_{3(g)}$), δ (ppm): 9.24 (d, $^3J_{H\text{-}H}$ = 4.2 Hz, 2H), 9.01 (d, $^3J_{H\text{-}H}$ = 4.7 Hz, 2H), 8.83-8.81 (m, 4H), 8.18 (d, $^3J_{H\text{-}H}$ = 8.2 Hz, 4H), 8.10 (d, $^3J_{H\text{-}H}$ = 8.2 Hz, 2H), 7.92 (d, $^3J_{H\text{-}H}$ = 8.2 Hz, 4H), 7.88 (d, $^3J_{H\text{-}H}$ = 8.2 Hz, 2H), 2.61 (s, 6H), -6.77 (s, 6H). MS (MALDI/TOF): *m/z* 815.67 $[M\text{-}DMSO]^{+\bullet}$, 815.86 calcd for $C_{37}H_{20}CoBr_3N_4$. HR-MS (ESI): m/z = 815.85748 $[M\text{-}DMSO]^{+\bullet}$, 815.85646 calcd for $C_{37}H_{20}CoBr_3N_4$.

Mono-(DMSO)cobalt [5,10,15-tris(4-fluorophenyl)]corrole, 7 was obtained as a red powder in 87% yield starting from the free base.[36] UV-vis (CH_2Cl_2 with 1% DMSO): λ_{max}, (nm) (ε x10^{-3} L mol^{-1} cm^{-1}) 387 (127.3), 565 (20.3). ^{1}H NMR (500 MHz, $CDCl_3$+$NH_{3(g)}$), δ (ppm): 9.23 (d, $^3J_{H\text{-}H}$ = 4.1 Hz, 2H), 9.00 (d, $^3J_{H\text{-}H}$ = 4.7 Hz, 2H), 8.81 (m, 4H), 8.26 (m, 4H), 8.17 (m, 2H), 7.50-7.42 (m, 6H), 2.61 (s, 6H), -6.77 (s, 6H). ^{19}F NMR (470 MHz, $CDCl_3$+$NH_{3(g)}$) δ -116.86 (s, 2F), -117.01 (s, 1F). MS (MALDI/TOF): *m/z* 635.72 $[M\text{-}DMSO]^{+\bullet}$, 636.10 calcd for $C_{37}H_{20}CoF_3N_4$. HR-MS (ESI): m/z = 636.09516 $[M\text{-}DMSO]^{+\bullet}$, 636.09666 calcd for $C_{37}H_{20}CoF_3N_4$.

Mono-(DMSO)cobalt [5,10,15-tris(3,4,5-trimethoxyphenyl)]corrole, 8 was obtained as pure red powder in 76% yield starting from the free base.[36] UV-vis (CH_2Cl_2 with 1% DMSO): λ_{max}, (nm) (ε x10^{-3} L mol^{-1} cm^{-1}) 406 (54.3), 563 (13.9). ^{1}H NMR (500 MHz, $CDCl_3$+ 5% $N_2H_4.H_2O$), δ (ppm): 9.17 (d, $^3J_{H-H}$ = 4.1 Hz, 2H), 9.10 (d, $^3J_{H-H}$ = 4.7 Hz, 2H), 8.89 (m, 4H), 7.51 (s, 4H), 7.43 (s, 2H), 4.11 (s, 9H), 4.01 (s, 12H), 3.95 (s, 6H), 2.57 (s, 6H), -3.91 (s, 4H). MS (MALDI/TOF): *m/z* 852.02 $[M\text{-}DMSO]^{+\bullet}$, 852.22 calcd for $C_{46}H_{41}CoN_4O_9$. HR-MS (ESI): m/z = 852.21998 $[M\text{-}DMSO]^{+\bullet}$, 852.22001 calcd for $C_{46}H_{41}CoN_4O_9$.

Mono-(DMSO)cobalt [5,10,15-tris(4-tertbutylphenyl)]corrole, 9 was obtained as a red powder in 90% yield starting from the free base.[36] UV-vis (CH_2Cl_2 with 1% DMSO): λ_{max}, (nm) (ε x10^{-3} L mol^{-1} cm^{-1}) 394 (94.3), 560 (16.4). ^{1}H NMR (500 MHz, $CDCl_3$+ 5% $N_2H_4.H_2O$), δ (ppm): 9.15 (d, $^3J_{H-H}$ = 4.2 Hz, 2H), 9.05 (d, $^3J_{H-H}$ = 4.7 Hz, 2H), 8.83-8.85 (m, 4H), 8.20 (d, $^3J_{H-H}$ = 8.0 Hz, 4H), 8.12 (d, $^3J_{H-H}$ = 8.0 Hz, 2H), 7.79 (d, $^3J_{H-H}$ = 8.0 Hz, 4H), 7.75 (d, $^3J_{H-H}$ = 8.0 Hz, 2H), 2.61 (s, 6H), 1.61 (s, 27H), -4.17 (s, 4H). MS (MALDI/TOF): *m/z* 750.16 $[M\text{-}DMSO]^{+\bullet}$, 750.32 calcd for $C_{49}H_{47}CoN_4$. HR-MS (ESI): m/z = 750.31228 $[M\text{-}DMSO]^{+\bullet}$, 750.31272 calcd for $C_{49}H_{47}CoN_4$.

Mono-(DMSO)cobalt [5,10,15-tris(4-methoxyphenyl)]corrole, 10 was obtained as pure red powder in 81% yield starting from the free base.[36] UV-vis (CH_2Cl_2 with 1% DMSO): λ_{max}, (nm) (ε ×10^{-3} L mol^{-1} cm^{-1}) 404 (78.0), 419 (79.0), 566 (15.5). ^{1}H NMR (500 MHz, $CDCl_3$+ 4% $N_2H_4.H_2O$), δ (ppm): 8.98 (d, $^3J_{H-H}$ = 4.1 Hz, 2H), 8.92 (d, $^3J_{H-H}$ = 4.7 Hz, 2H), 8.73 (d, $^3J_{H-H}$ = 4.7 Hz, 2H), 8.67 (d, $^3J_{H-H}$ = 4.1 Hz, 2H), 8.09 (d, $^3J_{H-H}$ = 8.0 Hz, 4H), 8.02 (d, $^3J_{H-H}$ = 8.0 Hz, 2H), 7.30 (d, $^3J_{H-H}$ = 8.0 Hz, 4H), 7.24 (d, $^3J_{H-H}$ = 8.0 Hz, 2H), 4.07 (s, 6H), 4.06 (s, 3H), 2.58 (s, 6H), -4.03 (s, 4H). MS (MALDI/TOF): *m/z* 671.81 $[M\text{-}DMSO]^{+\bullet}$, 672.16 calcd for $C_{40}H_{29}CoN_4O_3$. HR-MS (ESI): m/z = 672.15557 $[M\text{-}DMSO]^{+\bullet}$, 672.15662 calcd for $C_{40}H_{29}CoN_4O_3$.

RESULTS AND DISCUSSION

Synthesis of Cobalt Corroles. Synthesis and characterization of the free-base corroles **1H$_3$** to **10H$_3$** has been reported in the literature.[31-33, 36] The cobalt mono-DMSO adducts **1-10** were prepared by reaction of the **1H$_3$-10H$_3$** precursors with $Co(OAc)_2 \cdot 4H_2O$ as shown in Scheme 1 with the progress of the metalation being monitored by UV-visible spectroscopy and MALDI/TOF mass spectrometry after which the final cobalt corrole products were characterized by ^{1}H NMR, MS (MALDI/TOF) and HRMS (ESI). In each case, a perfect match was obtained between the theoretical and experimental mass values (see experimental section and Figures S1-S33). Proof of the DMSO coordination in compounds **1-10** is given by an NMR peak at 2.61 ppm in $CDCl_3$.

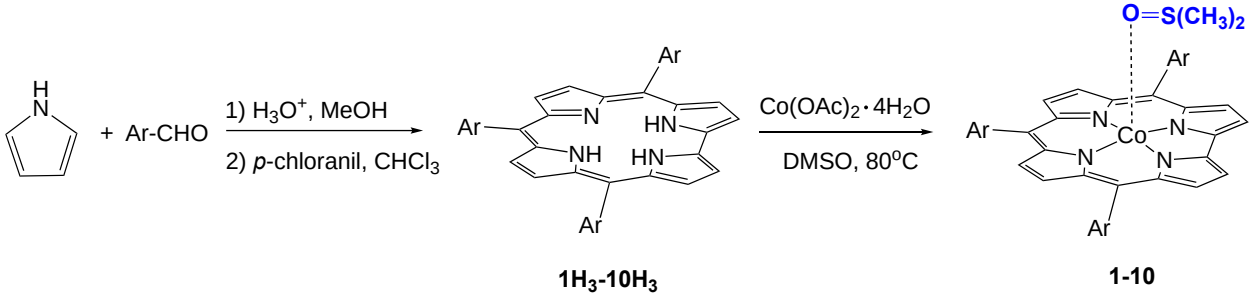

Scheme 1. Synthesis of mono-DMSO ligated cobalt corroles **1-10**.

UV-Visible Spectra under Electrochemical Conditions. Earlier spectral characterization of structurally related mono-DMSO corroles had shown that the DMSO ligand remained bound to the neutral compound when dissolved at millimolar concentrations in CH_2Cl_2 containing 0.1 M $TBAClO_4$ (the electrochemical conditions), while a dissociation of the DMSO axial ligand occurred in more dilute (10^{-5} M) solutions of the corrole in this solvent.[33] This concentration-dependent change in coordination number contrasted with what was seen in DMSO, where the mono-DMSO adduct was predominant for all concentrations of the compound, although a small

amount of bis-DMSO adducts seemed to be present for some of the examined corroles in this solvent.[33]

A similar solvent and concentration dependence on the cobalt coordination number is observed for the newly synthesized mono-DMSO adducts, whose spectra at 10^{-3} M in CH_2Cl_2 and DMSO containing 0.1 M $TBAClO_4$ are shown in Figure 1 and 2, where seven of ten examined compounds are characterized by a sharp Soret band at 377-393 nm when dissolved in CH_2Cl_2 at a 10^{-3} M concentration. The other three corroles are characterized by a broad band at 377 nm (compound **2**) or a split Soret band at 401-419 nm (compounds **8** and **10**). Nine of the ten examined corroles have a single Q band at 562–569 nm in CH_2Cl_2, the only exception being the F_5Ph substituted derivative **1**, which has shoulder bands at 535 nm and 569 nm. A summary of the spectral data in the two solvents is given in Table 1 and Figure 2.

The absorption bands of compounds **6-10** are only slightly dependent on solvent at a corrole concentration of 10^{-3} M (see Figure 2 and Table 1), and these spectra can be assigned in each case to a mono-DMSO adduct under the two solution conditions. This contrasts with compounds **2-5**, which are characterized by two absorption bands in the Soret region in DMSO, one at 375-393 and the other at 419-442 nm. There are also two Q bands for these compounds in DMSO, thus suggesting a mixture of the mono- and bis-(DMSO) adducts as also described in a previous study.[33] A complete formation of the bis-(DMSO) complex seems to occur for compound **1**, which contains three highly electron-withdrawing *meso*-F_5Ph groups. This species is characterized by a broad Soret band at 437 nm and two Q bands at 584 and 599 nm as seen in Figure 1b.

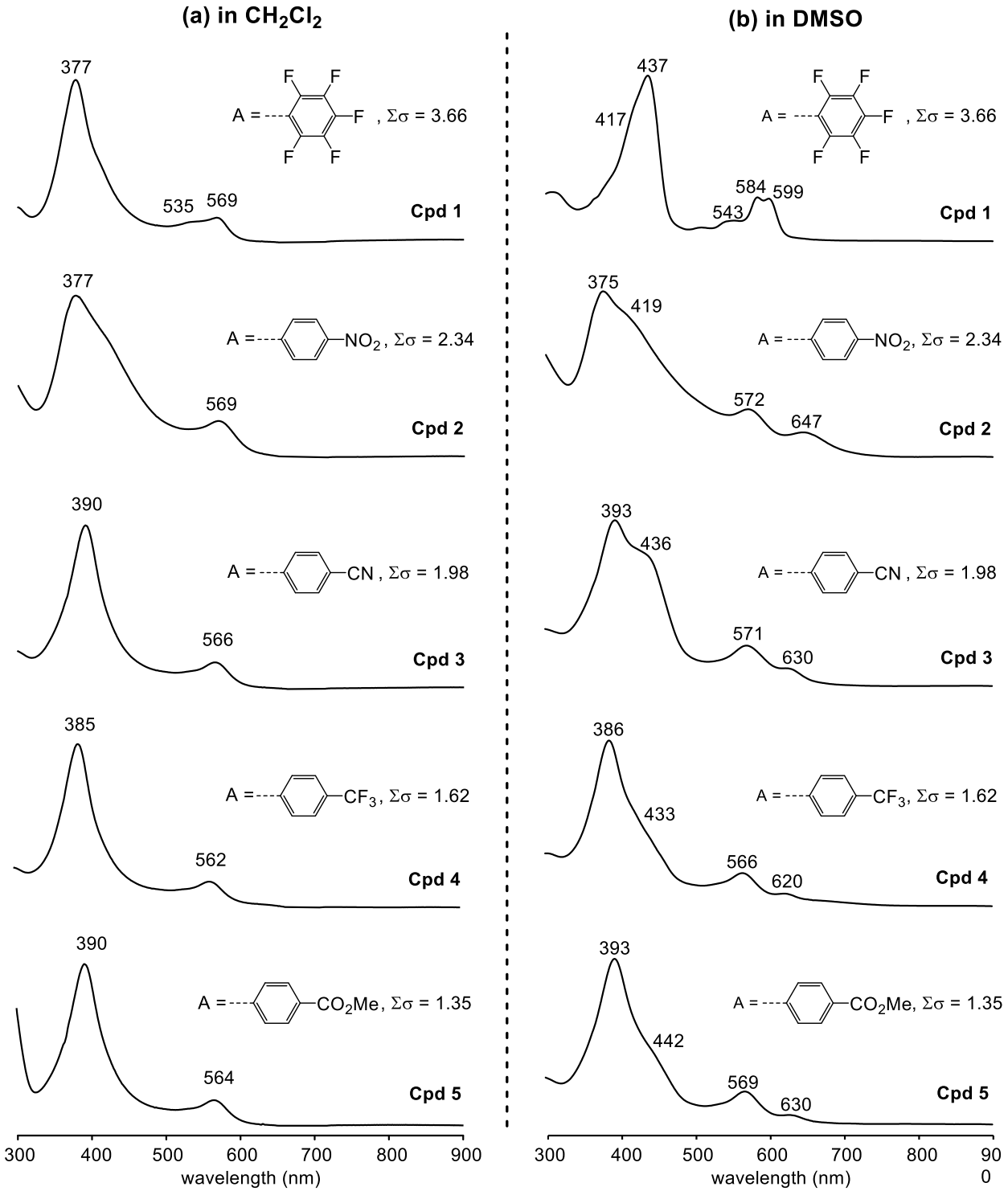

Figure 1. UV-visible spectra of compounds **1-5** at ~10^{-3} M in (a) CH_2Cl_2 and (b) DMSO, both containing 0.1 M $TBAClO_4$.

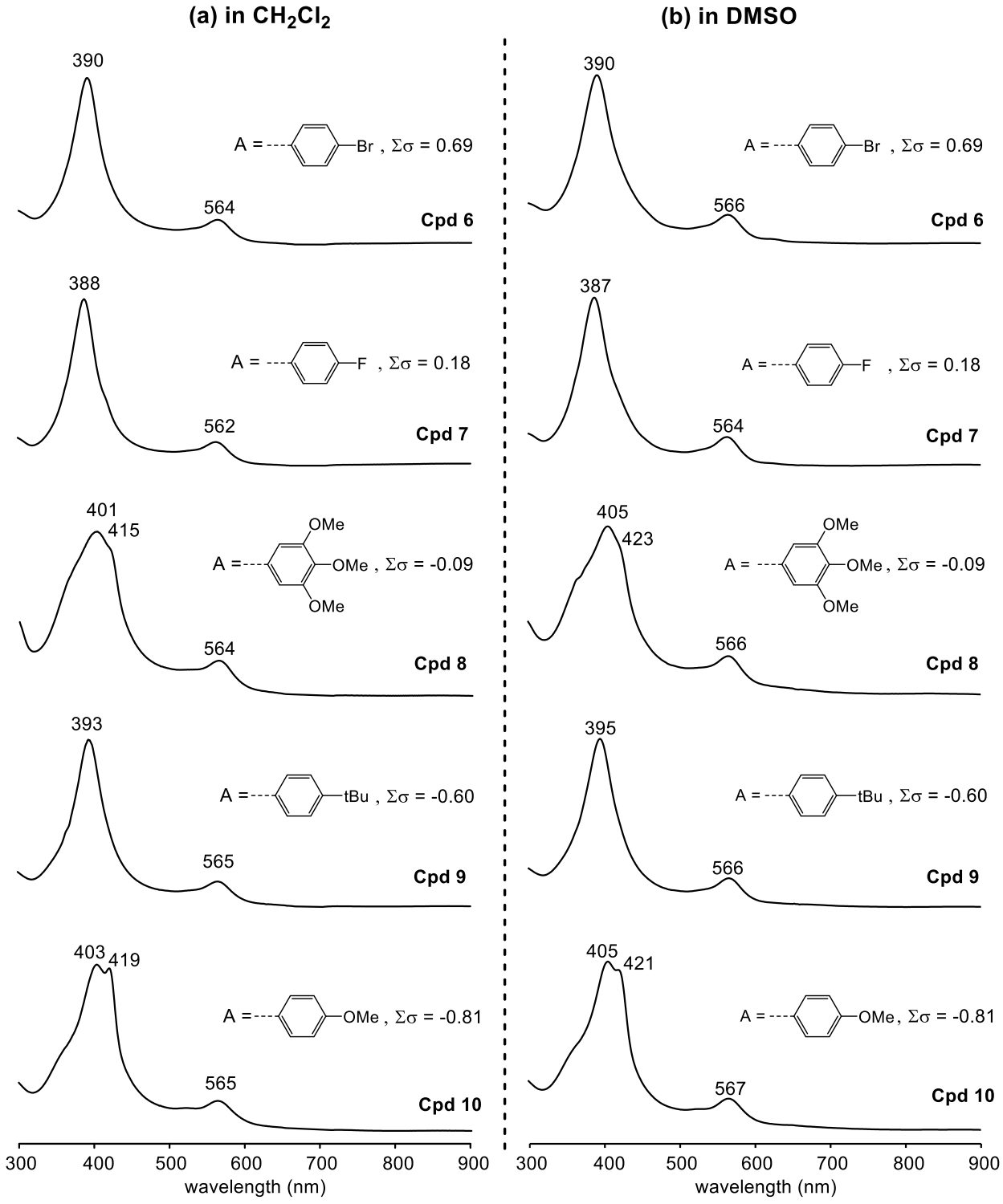

Figure 2. UV-visible spectra of compounds **6-10** at ~10^{-3} M in (a) CH_2Cl_2 and (b) DMSO, both containing 0.1 M $TBAClO_4$.

For some transition metal triarylcorroles, the position of the Soret and Q band maxima will vary with changes in the type of electron-donating or electron-withdrawing *meso*-substituents, while for others the Soret band remains relatively invariant with changes in the type of substituted *meso*-phenyl groups on the macrocycle. In the first case, the corrole can be assigned as having a non-innocent macrocyclic ligand, while in the second the compounds were said to have innocent macrocycles according to a criteria set forth by Ghosh.[2, 7, 18, 37-44]

The electrochemical data described later in the manuscript suggests a non-innocent macrocycle, but the above spectral diagnostic criteria of Ghosh for assigning ligand non-innocence to all of the investigated triarylcorroles cannot be reliably applied in the present study due to the fact that the coordination number of the neutral cobalt complexes varies from 4 (tetracoordinated) to 6 (hexacoordinated) with changes in the solution conditions, corrole concentration and specific electron-donating or withdrawing substituents on the *meso*-phenyl groups in the examined series of compounds.

Table 1. UV-visible spectral data of compounds **1-10** (~10^{-3} M) in CH_2Cl_2 and DMSO containing 0.1 M $TBAClO_4$.

compound		Solvent	λ_{max}, nm ($\varepsilon \times 10^{-4}$ M^{-1} cm^{-1})				
#	Ar		Soret region			visible region	
1	F_5Ph	CH_2Cl_2	377 (8.0)		535 (1.1)	569 (1.3)	
		DMSO	417[sh]	437 (6.2)	543 (0.7)	584 (1.7)	599 (1.6)
2	*p*-NO_2Ph	CH_2Cl_2	377 (6.0)[br]			569 (1.5)	
		DMSO	375 (4.3)	419 (3.5)[sh]		572 (1.3)	647 (0.7)
3	*p*-CNPh	CH_2Cl_2	390 (8.9)			566 (1.5)	
		DMSO	393 (4.8)	436 (3.8)[sh]		571 (1.2)	630 (0.5)
4	*p*-CF_3Ph	CH_2Cl_2	385 (8.2)			562 (1.5)	
		DMSO	386 (4.5)	433 (2.4)[sh]		566 (1.1)	620 (0.4)
5	*p*-CO_2MePh	CH_2Cl_2	390 (7.3)			564 (1.4)	
		DMSO	393 (5.8)	442 (2.7)[sh]		569 (1.3)	630 (0.5)
6	*p*-BrPh	CH_2Cl_2	390 (11.3)			564 (1.7)	
		DMSO	390 (7.2)			566 (1.3)	
7	*p*-FPh	CH_2Cl_2	388 (9.6)			562 (1.4)	
		DMSO	387 (6.0)			564 (1.0)	
8	*m*,*p*,*m*-$(OMe)_3Ph$	CH_2Cl_2	401 (4.7)	415 (4.3)		564 (1.1)	
		DMSO	405 (3.6)	423 (3.1)[sh]		566 (0.9)	
9	*p*-*t*BuPh	CH_2Cl_2	393 (11.1)			565 (1.9)	
		DMSO	395 (5.1)			566 (0.9)	
10	*p*-OMePh	CH_2Cl_2	403 (7.6)	419 (7.4)		565 (1.5)	
		DMSO	405 (5.3)	421 (5.1)[sh]		567 (1.0)	

[sh]shoulder peak; [br]broad peak.

UV-Visible Spectra of Dilute Corrole Solutions with and without Added Anions. In previous studies of structurally related cobalt triarylcorroles,[31-33] the four-coordinate compounds were spectrally characterized in dilute (10^{-5} M) solutions as possessing a single intense Soret band at about 390 nm and a weak Q band at about 540 nm, while the five-coordinate cobalt complexes with bound DMSO, CO or pyridine axial ligands had a lower-intensity Soret bands located at about 380 nm and a single Q band at about 560 nm.[33] Both spectral patterns are different from that of the six-coordinate corroles containing pyridine or NH_3 ligands, which display a split Soret band at about 435–450 nm and an intense Q band at 620 nm.[31, 32] Thus, a blue shift in the Soret-band maximum would be expected for a given cobalt triarylcorrole upon going from a 4- to a 5-coordinate complex, while a red shift with splitting of the Soret band and formation of a more intense Q band would be predicted to occur upon going from a 4- or 5- to a 6-coordinate complex.

This trend in the spectral patterns with changes in axial coordination seems to hold for the corroles examined in the current study, with examples being given in Figure 3 for compounds **1** and **6** at different concentrations in the two solvents. In the case of compound **1**, the Soret band shifts from 377 to 389 nm when decreasing the corrole concentration from 10^{-3} to 10^{-5} M in CH_2Cl_2, suggesting a dissociation of the single DMSO axial ligand in this solvent. This contrasts with what is seen in the DMSO solvent where the Soret band maximum is located at 437 or 438 nm independent of concentration, and is assigned to a 6-coordinate bis-DMSO adduct as described above.

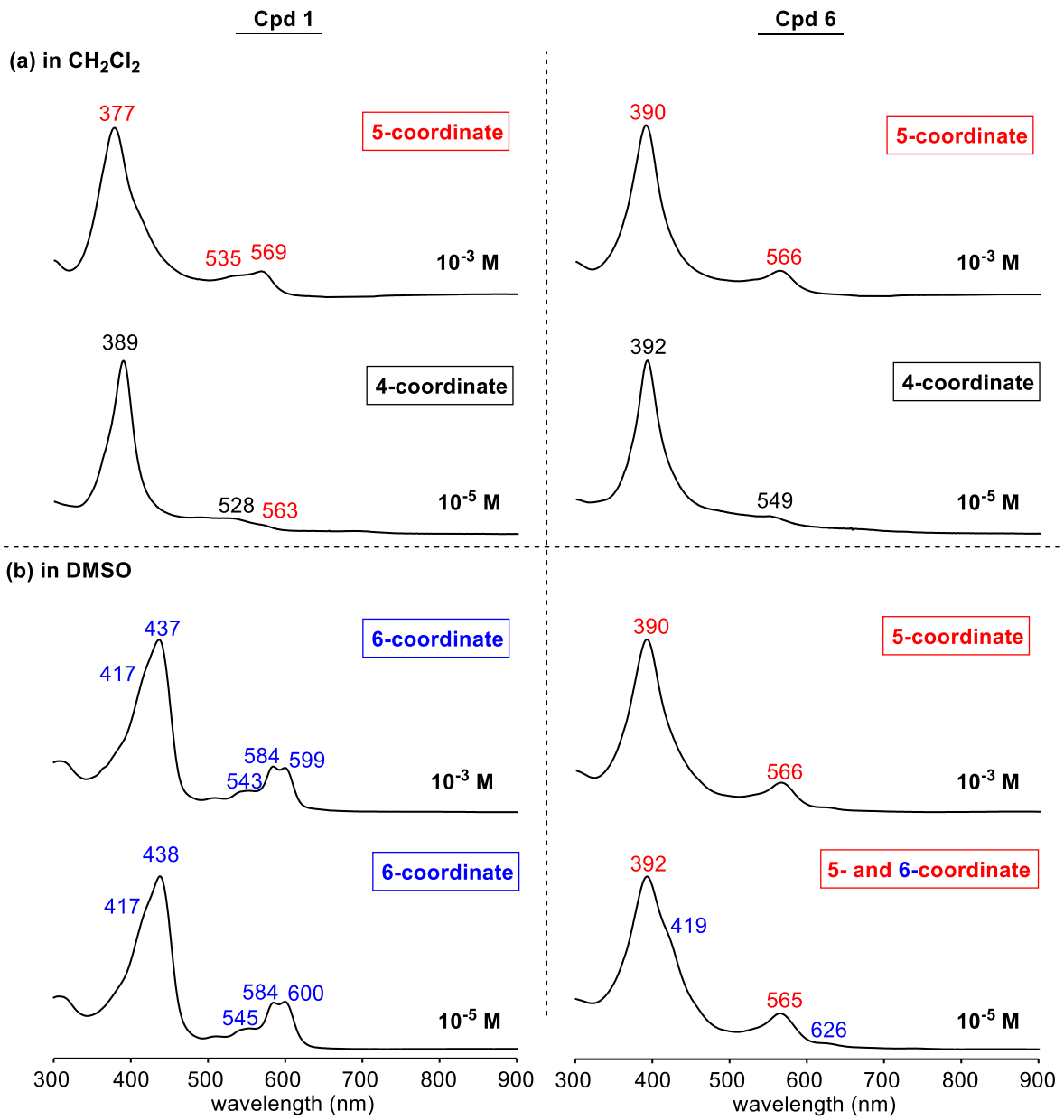

Figure 3. Concentration dependence on UV-visible spectra of compounds **1** and **6** in (a) CH_2Cl_2 and (b) DMSO.

The effect of anions on the UV-visible spectra of the corrole was investigated and examples are shown in Figure 4 for a 5.5 x 10^{-6} M solution of the compound **1** in CH_2Cl_2 containing different 0.1 M TBA^+X^- salts. Four groups of spectral patterns are observed and labelled as I, II, III and IV. The first group of spectra is in CH_2Cl_2 solutions containing 0.1 M PF_6^- or BF_4^- as well as in neat CH_2Cl_2 where the four coordinate corrole is characterized by a single Soret band at 388 nm and two Q bands at 528-531 and 563-565 nm. The second is in CH_2Cl_2 solutions containing the added HSO_4^-, ClO_4^-, Br^-, I^-, Cl^- or OAc^- anions, where there are two absorptions in the Soret region, one at 387-395 nm and the other at 404-419 nm. In solutions with OTs^- or F^-, the band at around 388 nm has totally disappeared and is replaced by an intense band at 418-419 nm and a new Q band at 610 to 633. This is the third spectral pattern. As will be described on the following pages the bands at 414-419 nm (as well as 404 nm for the Cl^- derivative) are assigned to a partially or fully reduced form of the corrole when in the presence of added anions.

Finally, a quite different spectrum is seen for compound **1** in CH_2Cl_2 solutions containing 0.1 M TBA^+CN^-. In this solution, three absorptions are seen in the Soret region (at 439-492 nm) and there is also an intense Q band at 667 nm, along with multiple weaker absorption bands from 553 to 620 nm. This spectrum is virtually identical to a spectrum reported by Gross and coworkers for the same A_3-corrole in CH_2Cl_2 solutions containing excess TBAOH.[45]

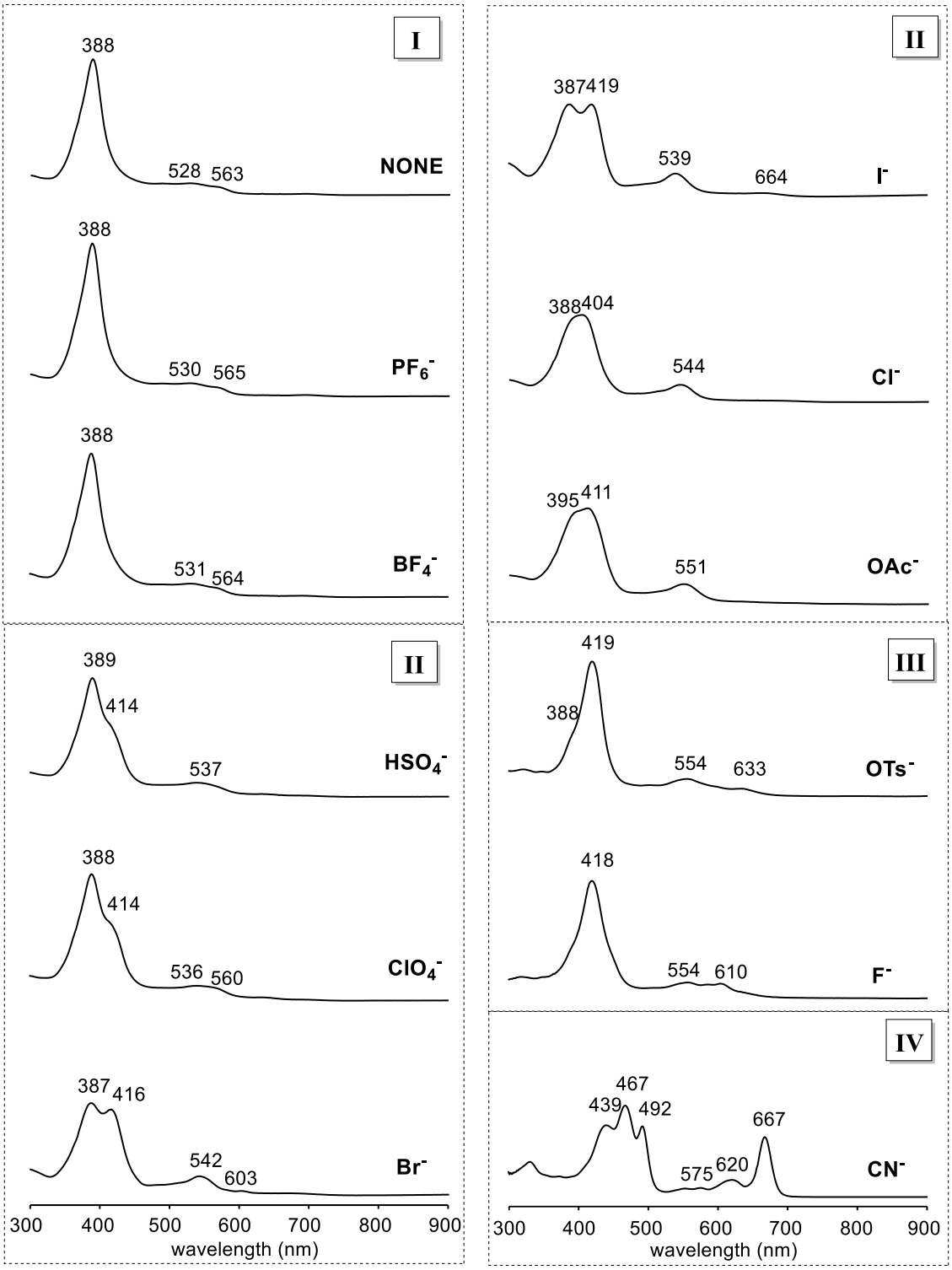

Figure 4. UV-vis spectra of compound **1** (5.5×10^{-6} M) in CH_2Cl_2 containing 0.1 M TBA^+X^- (X^- = PF_6^-, BF_4^-, HSO_4^-, ClO_4^-, Br^-, I^-, Cl^-, OAc^-, F^-, OTs^-, and CN^-).

Effect of Anions on the UV-visbile spectra in CH_2Cl_2. Selected corroles were spectroscopically monitored in CH_2Cl_2 during titrations with the anions in Chart 1. Examples of the spectral changes for compound **1** are shown in Figures 5a and 5b upon the stepwise addition of OAc^- and F^- to solution. The initial spectrum of compound **1** at a 10^{-5} M concentration in CH_2Cl_2 has a Soret band at 388 nm and two weak Q-band absorbances between 525 and 566 nm (see Figure 3a). This spectrum is assigned to the four-coordinate cobalt corrole which has lost the DMSO axial ligand at this concentration. However, after adding TBAOAc or TBAF to solution, the 388 nm band decreases in intensity and a new band is seen at 414 nm (for TBAOAc) or 418 nm (for TBAF). The reduced intensity and position of the Soret band after addition of these two anions is almost identical to what occurs upon electrochemical reduction, where λ_{max} varies between 419 and 426 nm depending upon the solvent and macrocycle, (see examples in references [22, 46] and Figure 5c for reduction of **1** in a thin layer cell). The spectrum in Figure 5b after addition of 50 eq TBAF to solution is also quite similar to what is observed for corroles **3-10** in CH_2Cl_2 containing 0.1 M TBAF in that there is a red-shifted Soret band between 415 and 429 nm, indicating a reduction in each case (Figure S34).

A reduction of the corrole by fluoride ion might be expected, given its reported ability to undergo anion-induced electron transfer through π-anion interactions,[47, 48] but it was totally unexpected that the weakly complexing tosylate anion would also enhance a reduction of the starting compound, as shown in Figure 4 for a 5.5 x 10^{-6} M corrole concentration in 0.1 M TBAOTs. However, it should be noted that the reduction with tosylate is slow, as shown in Figure 6 for compound **7** at a concentration of 4.6 x 10^{-6} M. The slow conversion between the two forms of the corrole is consistent with a rate determining chemical reduction of the $Cor^{+\bullet}$ in solution. The final generated cobalt(II) corrole spectrum in CH_2Cl_2 solutions with tosylate has a Soret band at 420 nm

for **7** (Figure 6) and 419 nm and two Q-bands at 576 and 626, features which are also seen for the electrochemically reduced corrole **1** in CH_2Cl_2 containing 0.1 M $TBAClO_4$ (Figure 5c).

In contrast to reduction of the corrole, which occurs in CH_2Cl_2 solutions containing fluoride or tosylate anions, the addition of TBACN leads to a bis-cyanide adduct of the neutral corrole as shown in Figure 7 for compound **1**. The ligand addition is stepwise, with the first step being complete after the addition of just one equivalent of CN^-, giving a spectrum with absorptions at 414, 552 and 580 nm. The position of the Soret band at 414 nm resembles that for the final spectrum of the chemically reduced corrole in solutions containing OTs^- or F^- (Figures 5 and 6), but the spectrum after addition of 1 eq. CN^- lacks the diagnostic broad Q-band of the singly reduced species at 626-631 nm (Figure 5b,c and Figure 6) and is unambiguously assigned to the mono-ligated neutral corrole. The log K_1 value for addition of the first CN^- group to compound **1** is too large to be determined by a diagnostic log-log Hill plot, but this is not the case for addition of the second CN^- axial ligand, where K_2 was measured as $10^{4.3}$ as shown in the insert of Figure 7b. Three isosbestic points are seen in the figure indicating the presence of only two spectroscopically detectable species in solution. The final spectrum of the assigned bis-CN adduct has three bands at 438, 466 and 491 nm as well as Q bands at 621 and 667 nm, the latter of which is intense and a diagnostic marker band for formation of the six-coordinate cobalt corrole.[31]

Similar two-step spectral changes are also seen during titrations of the other corroles with CN^- and attempts are now being made to isolate the initial and final products for further characterization.

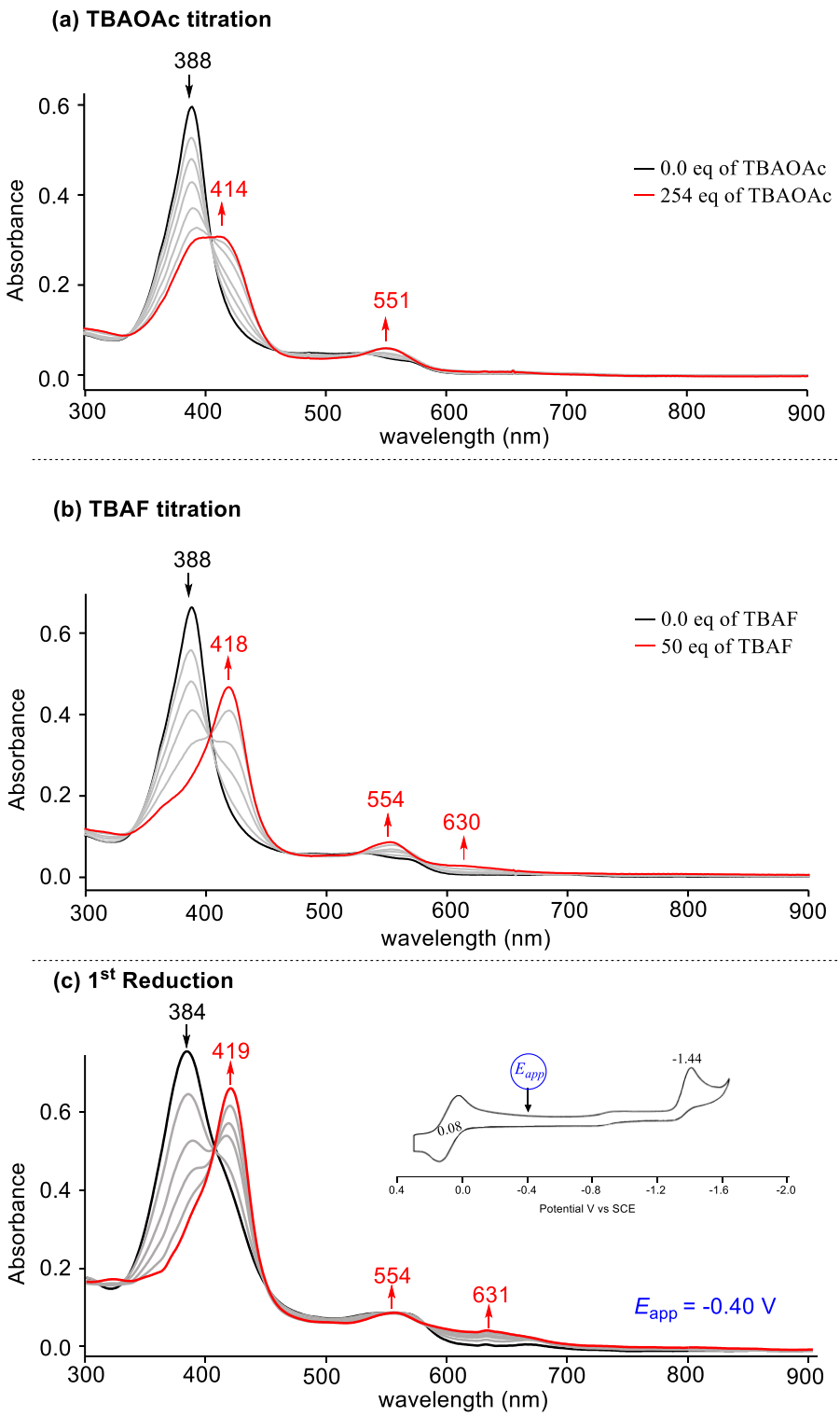

Figure 5. UV-vis spectral changes of compound **1** $(F_5Ph)_3CorCo(DMSO)$ (~10^{-5} M) titrations of (a) TBAOAc and (b) TBAF in CH_2Cl_2 and for (c) electroreduction (~10^{-4} M) in CH_2Cl_2 containing 0.1 M $TBAClO_4$.

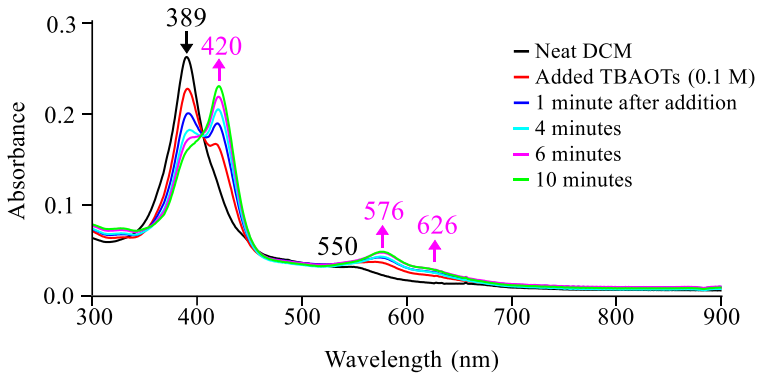

Figure 6. Time dependent UV-vis spectral changes of compound **7** at 5×10^{-6} M after addition of 0.1 M TBAOTs to a CH_2Cl_2 solution.

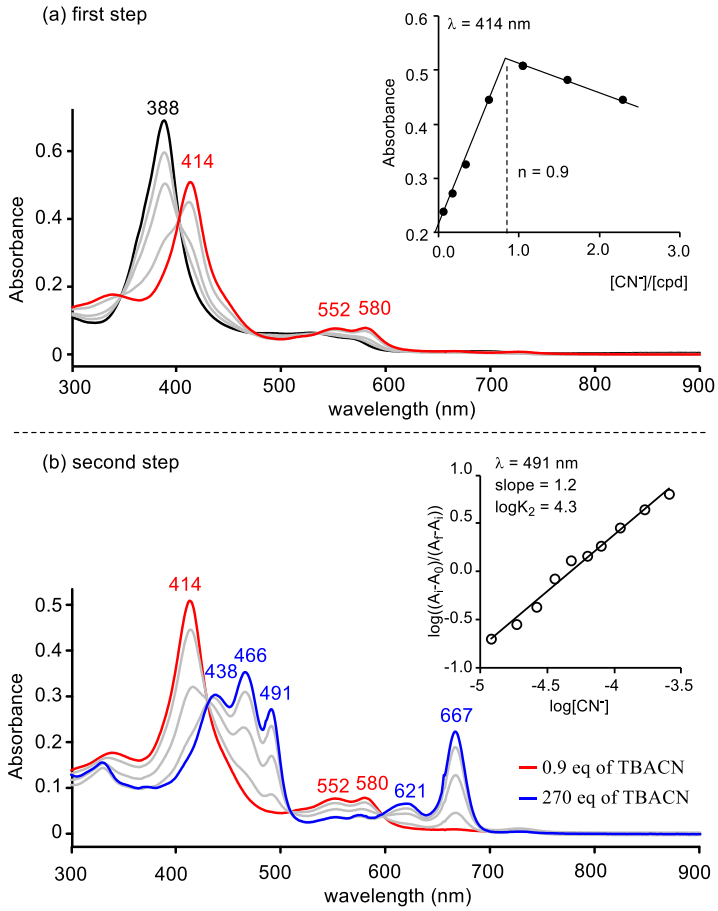

Figure 7. UV-vis spectral changes of compound **1** (1.2×10^{-5} M) in CH_2Cl_2 titrated with TBACN.

Electrochemistry in Solutions Containing 0.1 M $TBAClO_4$. Cyclic voltammograms of corroles **1-10** were obtained in CH_2Cl_2 and DMSO containing 0.1 M $TBAClO_4$. Examples for two of the corroles (**1** and **5**) are shown in Figures 8 and a summary of the measured half-wave potentials is given in Table 2. Voltammograms for each corrole in the two solvents are illustrated in Figures S35-S38.

As shown in the Figure 8, two or three oxidations and two reductions can be seen for each corrole within the solvent potential limit. The first reduction is reversible in both DMSO and CH_2Cl_2, but this is not the case for the second electron addition in CH_2Cl_2, where a homogenous chemical reaction follows the second reduction[22] located at E_{pc} = -1.44 V (for **1**) or -1.55 V (for **5**). A reaction with the solvent does not occur in DMSO, where the second reductions are all reversible and located at $E_{1/2}$ values between -1.42 (for **1**) and -1.67 (for **10**) (see Table 2). A third irreversible reduction is also seen for compound **1** at E_{pc} = -1.82 V, when the reaction is carried out in CH_2Cl_2 (Figure 8). This process does not occur in DMSO and is assigned to the product from the coupled chemical reaction involving the doubly reduced species.

Compound **2** also has a different redox behavior than the other corroles, due to the presence of the three electroreducible *meso*-NO_2Ph substituents.[31, 33] The first reversible reduction of the three NO_2Ph groups is seen at $E_{1/2}$ = -1.14 V in CH_2Cl_2 (Figure S34) and -1.12 V in DMSO (Figure S35) and a further reduction of these groups is located at -1.95 V, a result consistent with data earlier reported in the literature.[31, 33]

An "extra" redox process can also be seen for compound **8** at 0.07 V in CH_2Cl_2 and 0.05 V in DMSO (Figure S36). Overlapping oxidation processes can be seen for corroles **8-10** in CH_2Cl_2 (Figure S36).

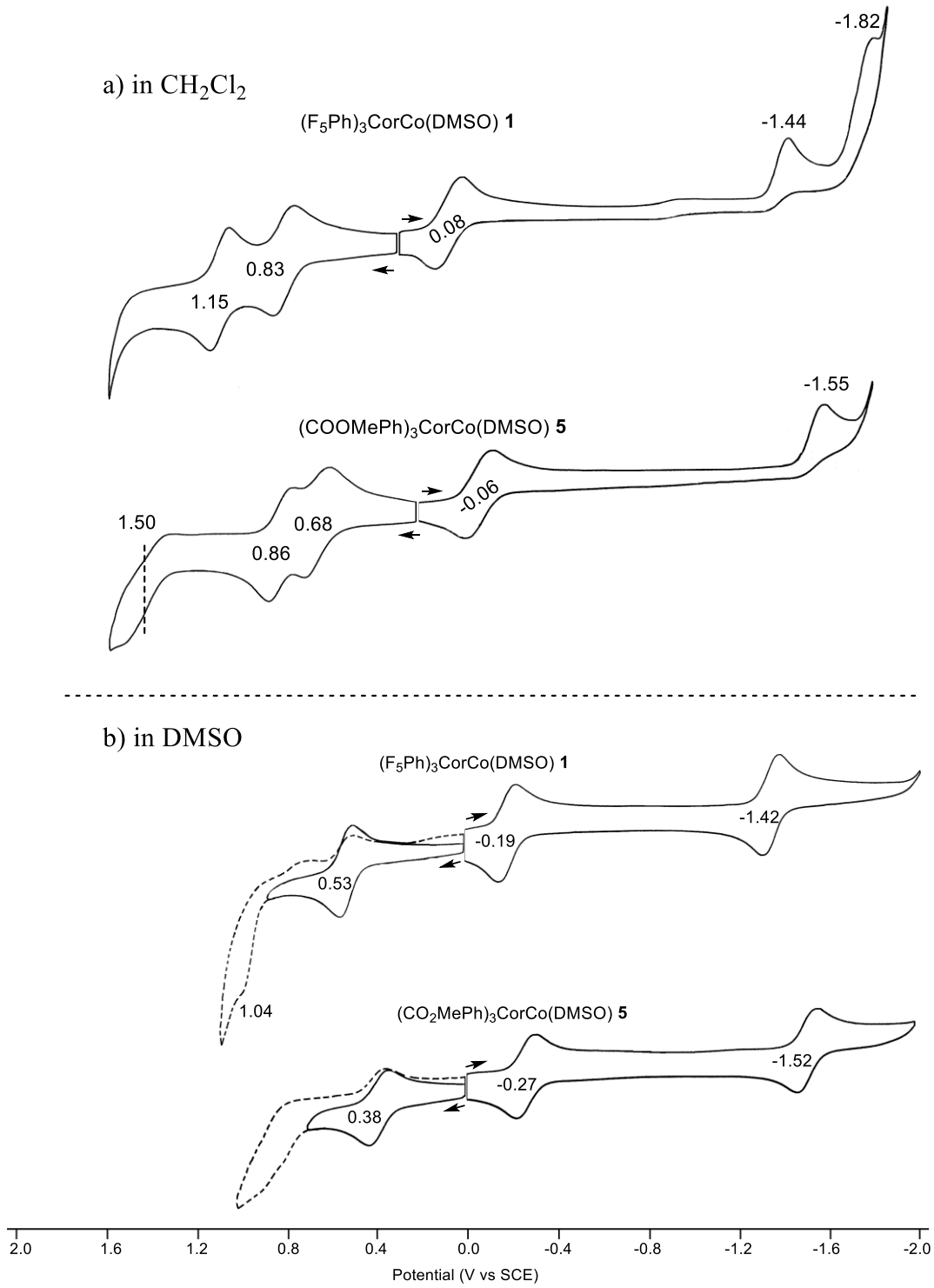

Figure 8. Cyclic voltammograms of compounds **1** and **5** in a) CH_2Cl_2 and b) DMSO containing 0.1 M $TBAClO_4$.

Table 2. Half-wave or peak potentials ($E_{1/2}$ or E_p, V vs SCE) of **1-10** in CH_2Cl_2 and DMSO containing 0.1 M $TBAClO_4$.

cpd	3σ[a]	Solvent	Potentials (V vs SCE)					
			Ox 3	Ox 2	Ox 1	Red 1	Red 2	Red 3
1	3.66	CH_2Cl_2	-	1.15	0.83	0.08	-1.44[b]	-1.82[b]
		DMSO		1.04[b]	0.53	-0.19	-1.42	
2	2.34	CH_2Cl_2	1.55	0.89	0.73	0.00	-1.14[c]	-1.75[d]
		DMSO		1.02[b]	0.41	-0.22	-1.12[c]	-1.94[d]
3	1.98	CH_2Cl_2	1.55	0.89	0.72	-0.03	-1.50	
		DMSO	1.01[b]	0.92[b]	0.41	-0.23	-1.47	
4	1.62	CH_2Cl_2	1.51	0.87	0.69	-0.06	-1.56[b]	
		DMSO	0.98[b]	0.88[b]	0.39	-0.27	-1.53	
5	1.35	CH_2Cl_2	1.50	0.86	0.68	-0.06	-1.55[b]	
		DMSO			0.38	-0.27	-1.52	
6	0.69	CH_2Cl_2	1.49	0.85	0.68	-0.08	-1.56[b]	
		DMSO		0.79	0.35	-0.30	-1.58	
7	0.18	CH_2Cl_2	1.49	0.82	0.65	-0.13	-1.63[b]	
		DMSO		0.77	0.35	-0.33	-1.61	
8	-0.09	CH_2Cl_2	-	0.75	0.60	0.07, -0.16	-1.63[b]	
		DMSO		0.75	0.35	-0.32	-1.62	
9	-0.60	CH_2Cl_2	1.40, 1.52	0.76	0.56	-0.17	-1.68[b]	
		DMSO		0.62	0.32	-0.36	-1.66	
10	-0.81	CH_2Cl_2	1.38	0.73	0.55	-0.16	-1.67[b]	
		DMSO	0.90	0.68	0.31	-0.38	-1.67	

[a] Hammett values taken from ref [49, 50]. Peak potential (E_{pc} for reduction and E_{pa} for oxidation). [c]First one-electron reversible reduction for nitrophenyl groups. [d]Further multi-electron reductions for nitrophenyl group may overlap with the second cobalt corrole reduction.

The measured potentials for each redox reaction of corroles **1-10** in DMSO and CH_2Cl_2 containing 0.1 M TBAP are given in Table 2 and are consistent with earlier reported values for mono-DMSO adducts of structurally related cobalt corroles in these two solvents, namely the first reduction is harder and the first oxidation easier for a given compound in DMSO than in CH_2Cl_2. This is graphically seen in Figure 8 where $E_{1/2}$ for the first one-electron reduction of compounds **1**

and **5** is shifted negatively in DMSO by 270 and 210 mV as compared to CH_2Cl_2 and a larger 300 mV negative shift in $E_{1/2}$ is seen for the first oxidation of the same two corroles upon going from CH_2Cl_2 containing 0.1 M $TBAClO_4$ (0.83 and 0.68 V) to DMSO containing 0.1 M $TBAClO_4$ (0.53 and 0.38 V). At the same time, the potentials for the second electron addition are effectively unchanged with solvent, being located at E_p = -1.44 V or $E_{1/2}$ = -1.42 V for compound **1** and E_p = -1.55 V or $E_{1/2}$ = -1.52 V for compound **5**.

The half wave potentials for each redox reaction of **1-10** also vary directly with the electron-donating or withdrawing effects of the *meso*-phenyl substituents. This has been illustrated numerous times by electrochemical free-energy relationships of *meso*-substituted porphyrins[51-54] and corroles,[8, 46, 55-57] where the reversible $E_{1/2}$ values were plotted *vs* the sum of the Hammett substituent constants of the macrocycle to determine both the consistency of the electron transfer mechanism over a given series of compounds and the degree of interaction between the substituent and the electron transfer rate.

As expected, measured potentials for the currently examined corroles are linearly related to the electron-withdrawing or electron-donating properties of substituents located on the three *meso*-phenyl rings of the corrole. Examples of these diagnostic linear free energy plots are given in Figure 9 for the two reversible reductions and one reversible oxidation of the corroles in DMSO. The compound numbers are given in Figures 9 and 10 and the individually measured potentials and the sum of the Hammett substituent constants (3σ) are given in Table 2.

The slopes of the $\Delta E_{1/2}/3\sigma$ (the ρ values) plots for the electrode reactions in DMSO are 43 and 53 mV for reduction and 42 mV for oxidation and slightly larger slopes are obtained for the related redox reactions in CH_2Cl_2 (Figure 10), where ρ = 53 and 55 mV for the two reductions and 58 mV for the oxidation. The linearity in the $E_{1/2}$ vs 3σ plots and the almost identical magnitude

of the slopes for the three redox reactions in a given solvent indicate no change in the reduction or oxidation mechanism for each electrode reaction throughout the series. It also indicates an almost identical interaction of the *meso* substituents with the electron transfer site in each case.

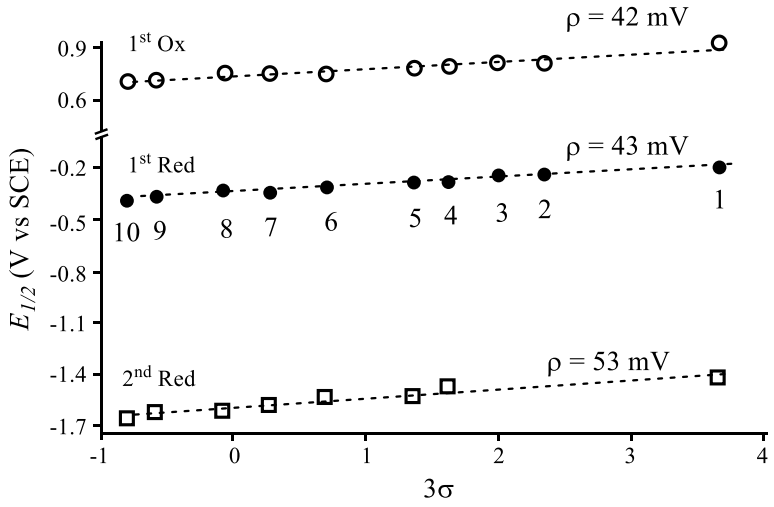

Figure 9. Plots of half-wave potentials vs 3σ in DMSO containing 0.1 M $TBAClO_4$. The values of potentials are given in Table 2 and the compound numbers are indicated in the figure. The second reduction of **2** has been excluded (see text).

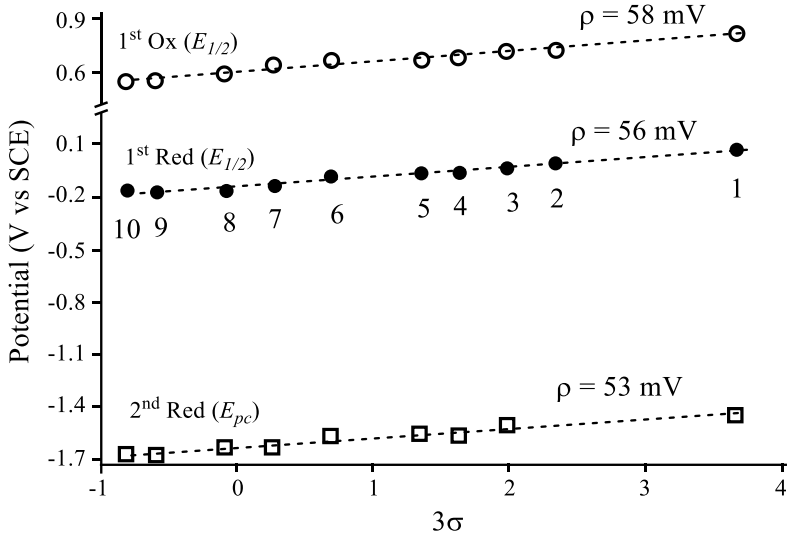

Figure 10. Plots of half-wave potentials or peak potentials vs 3σ in CH_2Cl_2 containing 0.1 M $TBAClO_4$. The values of potentials are given in Table 2 and the compound numbers are indicated in the figure. The second reduction of **2** has been excluded (see text).

Effect of Anions on the Electrochemistry in CH_2Cl_2. To investigate the effect of anions on half-wave potentials, the electrochemistry of compound **6** was characterized in CH_2Cl_2 containing 0.1 M TBA^+X^-, where $X^- = PF_6^-$, ClO_4^-, Br^-, Cl^-, F^-, or CN^-. Three distinct patterns of cyclic voltammograms can be seen in solutions containing these anions. The first is shown in Figure 11a for CH_2Cl_2 solutions containing PF_6^- and ClO_4^-. The second is in Figure 11b for solutions containing 0.1 M Br^- and Cl^- anions, while the third is given in Figure 11c for a CH_2Cl_2 solution of compound **6** containing F^- anion.

The large (410-450 mV) negative shift in $E_{1/2}$ for the two reversible corrole oxidations in solutions containing Br^- and Cl^- (Figure 11b) is similar to what occurs when DMSO binds to the 4 coordinate oxidized form of the corrole, as reported in the literature for related corroles,[33] and also in Figure 8 and Table 2 for the currently investigated derivatives. An absence of anion binding to the neutral corrole in CH_2Cl_2 at concentrations of 10^{-3} M is strongly suggested by the nearly identical $E_{1/2}$ values for the first reduction in solutions containing TBAX, where $X = PF_6^-$, ClO_4^-, Br^- and Cl^- (Figures 11a and b).

As spectroscopically demonstrated in Figures 5b and S34, a reduction of the cobalt corrole at ~10^{-5} M is observed in solutions with 0.1 M TBAF. A similar fluoride-induced reduction of the corrole also occurs at an electrochemical concentration of 10^{-3} M, where the redox active species in solutions of compounds **1-10** is actually that of the singly reduced monoanionic species. Under these conditions, the $[CorCo]^0$ to $[CorCo]^-$ process involves the conversion of $[CorCo]^-$ to $[CorCo]^0$ at the electrode surface, i.e an oxidation is observed rather a reduction. Nonetheless, the reversible potential for this redox process is 0.00 V, a value not so different than that for reduction of the same corrole in the presence of the four other anions in Figure 11.

Further proof for this assignment of the redox process is given by the spectroelectrochemical data presented in Figure 12a and 12b for compound **6** where the neutral corrole is characterized by a Soret band at 391 nm (X = ClO_4^-) or 399 nm (X = Cl^-), while the electrochemically generated species has a red-shifted Soret band at 424 or 425 nm after reduction at -0.60 V in the thin-layer cell. This contrasts with what is obtained for solutions of the same corrole containing 0.1 M TBAF (Figure 12c), where the Soret band in the absence of an applied potential is located at 422 nm and no change occurs when a reducing potential of -0.60 V is applied. However, a slight blue-shift and decrease in intensity of the initial Soret band is observed upon application of a controlled oxidizing potential in the thin layer cell. The final spectrum with λ_{max} = 415 nm is not that of the neutral corrole, but is rather a mixture of the reduced and neutral form of the corrole owing to the large excess of the anion reductant which does not allow for a complete regeneration of the $[CorCo]^0$ species.

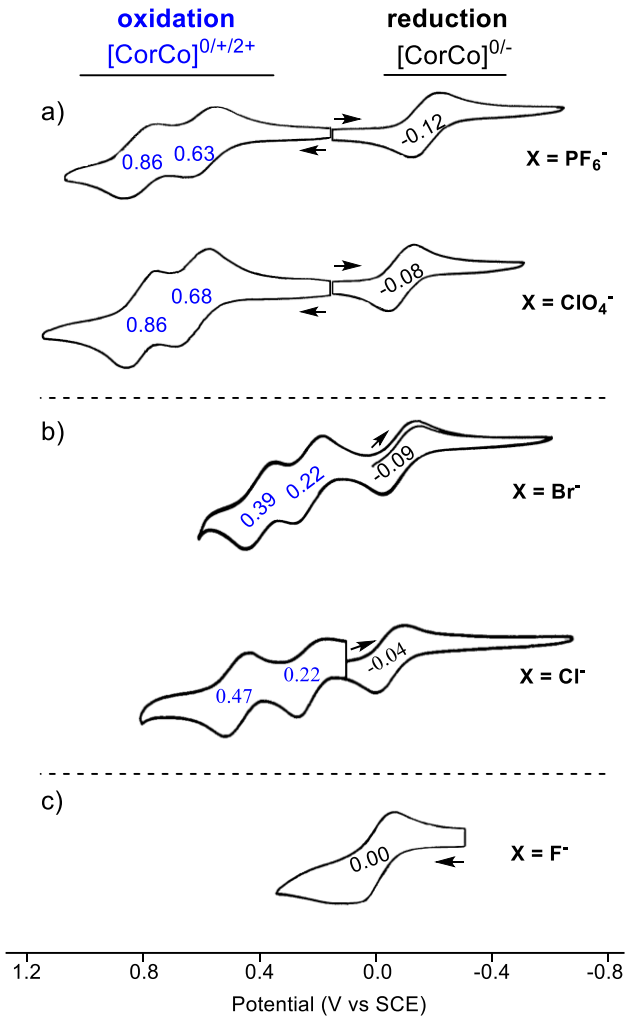

Figure 11. Cyclic voltammograms of compound **6** (10^{-3} M) in CH_2Cl_2 containing 0.1 M TBAX (X = PF_6^-, ClO_4^-, Br^-, Cl^-, F^-) and grouped by a) weakly coordinating anions, b) strongly coordinating anions and c) a reducing anion.

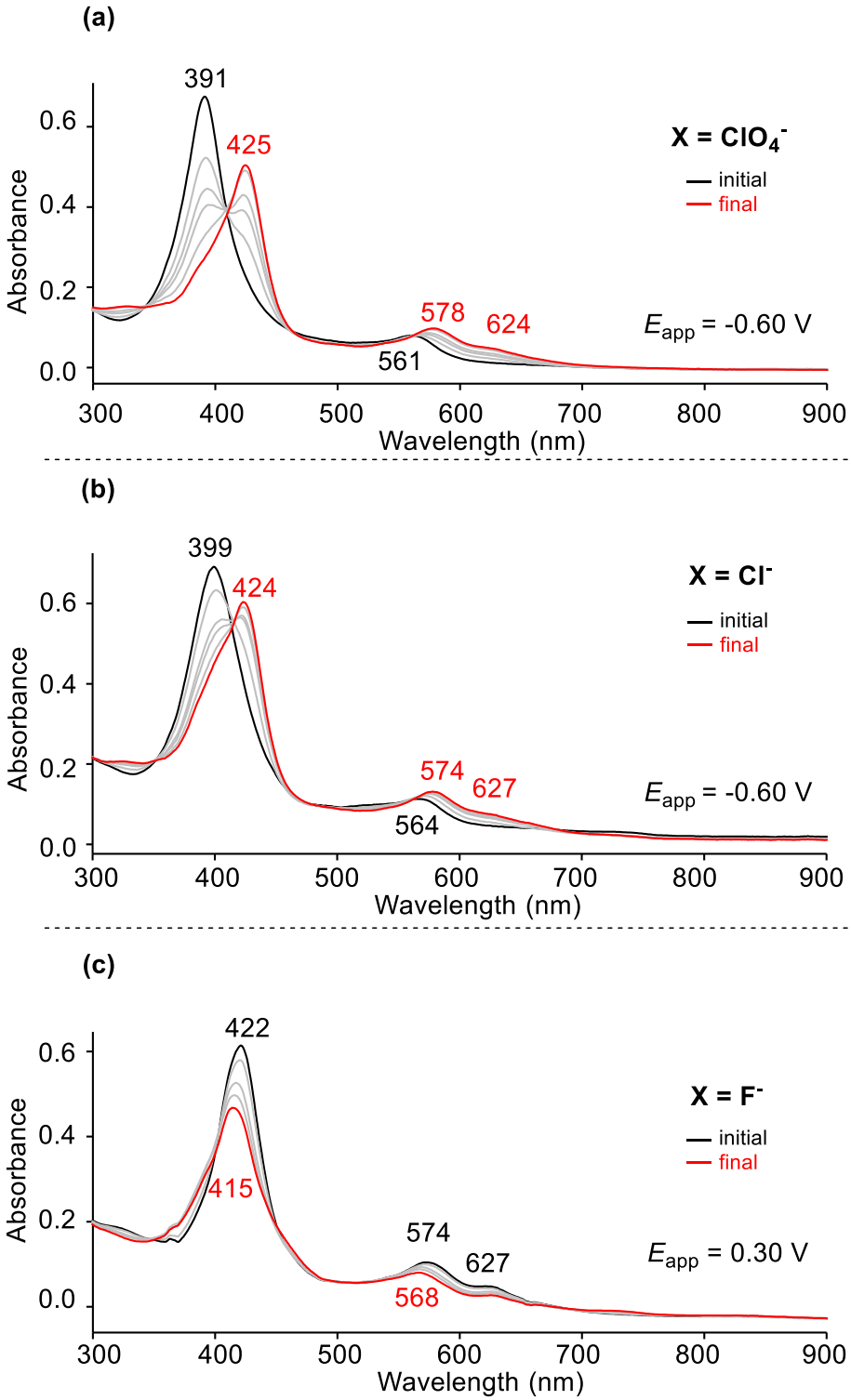

Figure 12. UV-visible spectral changes of compound **6** (10^{-4} M) during controlled potential reductions in CH_2Cl_2 containing a) 0.1 M $TBAClO_4$, b) 0.1 M TBACl and c) 0.1 M TBAF. The initial spectra are indicated in black and spectra for the products of the electrochemical reaction are in red.

Like the fluoride anion, CN^- can also act as reductant,[47] but one key difference in the present study is the ability of CN^- to coordinate with the neutral form of the investigated corroles, a feature not seen for any of the other investigated anions in the current study. The lack of binding by the other anions to compounds **1-10** in their neutral form is evident by the negligible shift in the first reduction potential in solutions containing 0.1 M TBAX, where X is any of the anions in Chart 1 except for CN^- (see examples in Figure 11).

If one of the examined anions were to complex the neutral, but not the singly reduced corrole one would expect to observe a 60 mV cathodic (negative) shift in $E_{1/2}$ for each 10 fold increase in anion concentration in solution, but this is not observed for any anion except for cyanide. In the case of CN^-, a titration of the corrole with TBACN results in a loss of current for the initial facile reduction process and the appearance of a new reduction process at potentials more negative than -1.0 V vs SCE. This is much like what has been reported for titrations of related cobalt corroles with pyridine.[31]

At the same time, the first reversible oxidation of the corrole, located at 0.67 V for compound **6** in solutions of ClO_4^- (and 0.22 V in solutions of Br^- or Cl^-, Figure 11) is shifted to -0.27 V in CH_2Cl_2 containing 0.1 M TBACN (see inset in Figure 13). The $E_{1/2}$ for this process does not vary with changes in cyanide concentration (see Figure S39 for an example), thus indicating that the same number of CN^- ligands are complexed to the initial and singly oxidized forms of the corrole, giving an oxidation reaction as described in eq 3.

$$[(Ar)_3CorCo^{III}(CN)_2]^- \rightleftharpoons (Ar)_3Cor^{\bullet}Co^{III}(CN)_2 + e^- \quad (3)$$

Further evidence for the assignment in eq. 3 is given by the spectroelectrochemical data for compound **6** in CH_2Cl_2 containing 0.1 M TBACN (Figure 13). The bis-CN adduct undergoes

no spectral changes under the application of a reducing potential as occurs for CH_2Cl_2 solutions containing 0.1 M $TBAClO_4$ or TBACl (Figures 12a and b) but a rapid spectral change is seen under an applied oxidizing potential of 0.20 V in the thin layer cell (Figure 13), giving a final spectrum with a broad Soret band at 440 nm and a near IR band a 741 nm. Two well-defined isosbestic points are obtained in the conversion of $[(Ar)_3CorCo(CN)_2]^-$ to $(Ar)_3Cor^{\bullet}Co(CN)_2$ and the spectral features of the final species generated at 0.20 V are quite similar to previously reported spectra for singly oxidized cobalt triarylcorroles in solutions of 0.1 M TBACl. These spectra were assigned to a Co^{III} corrole π-cation radical.[22, 34]

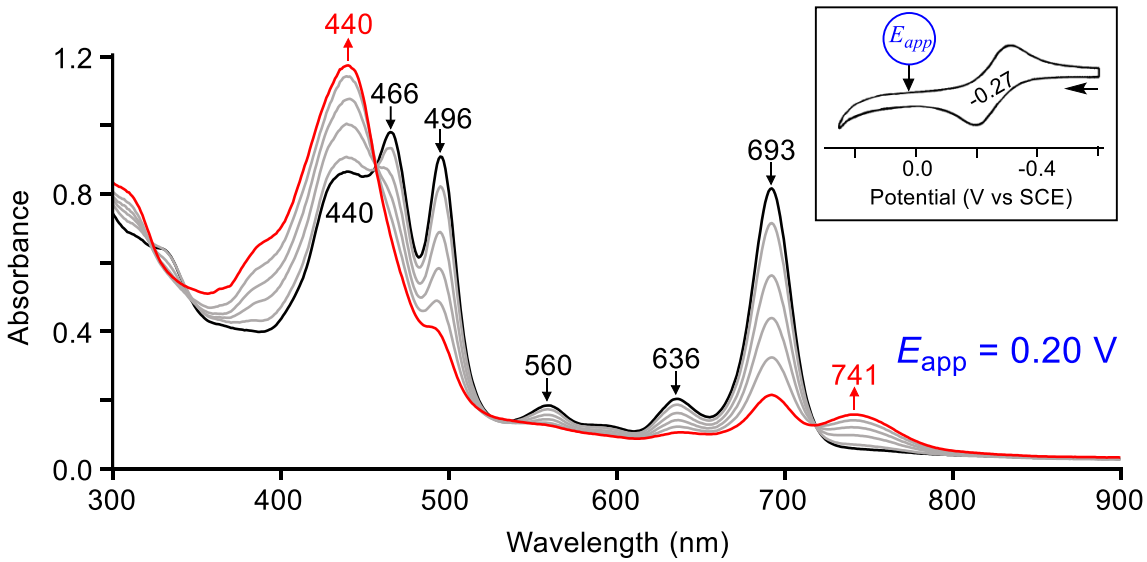

Figure 13. Spectral changes during oxidation of the bis-CN adduct of compound **6** at an applied potential of 0.20 V in CH_2Cl_2 containing 0.1 M TBACN. The cyclic voltammogram under these solution conditions is shown in the inset.

Bis-CN cobalt(III) complexes were also generated for the other corroles in this study by the addition of TBACN and like in the case of compound **6** described above, the measured halfwave potentials were independent of the concentration of CN^- added to solution once $[(Ar)_3CorCo(CN)_2]^-$ was formed. This required only 4-5 equivalents of TBACN being added to

solution, after which cyclic voltammograms showed a single reversible oxidation were obtained as illustrated in Figure 14 for corroles **1**, **6**, **7** and **10** in CH_2Cl_2. The reversible potential for the one-electron oxidation of $[(Ar)_3CorCo(CN)_2]^-$ varied from $E_{1/2}$ = 0.00 V for **1** to $E_{1/2}$ = -0.42 V for compound **10** in CH_2Cl_2 containing >5 eq. of TBACN. Once the bis-CN adduct was generated, the first reduction at 0.08 V (for **1**) or -0.16 V (for **10**) was shifted negatively to values beyond the potential range of the in CH_2Cl_2 solvent, thus indicating a strong stabilization of the cobalt(III) oxidation state in the bis-CN derivative.

Finally, it is interesting to point out that the first reversible ring-centered *reduction* of **6** according to eq 1 is located at a potential of $E_{1/2}$ = -0.08 V in CH_2Cl_2 containing 0.1 M $TBAClO_4$, while the first ring-centered *oxidation* of the same macrocycle in CH_2Cl_2, 0.1 M TBACN occurs at $E_{1/2}$ = -0.27 V according to eq 3. The solution conditions and metal oxidation states are different for the two reactions, but one might (in error) report a "negative" HOMO-LUMO gap of -0.19 V, a ludicrous concept but one that defines the electrochemical gap as the absolute potential difference between $E_{1/2}$ values for the first ring oxidation and the first ring reduction at the conjugated macrocycle.

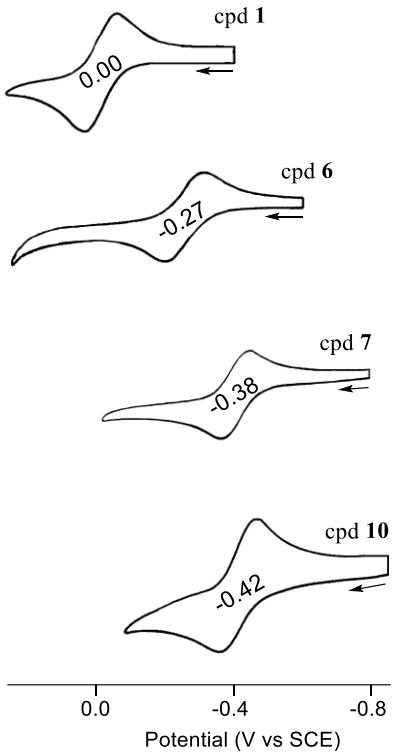

Figure 14. Cyclic voltammograms of corroles **1**, **6**, **7**, and **10** at 10^{-3} M in CH_2Cl_2 containing 0.1 M $TBAClO_4$ with >5 eq. TBACN.

Attempts are now being made to isolate and structurally characterize the mono- and bis-CN adducts of compounds **1-10** in the solid state and to also better elucidate the influence of cyanide axial ligands on the electrochemical processes and innocence or noninnocence of the corrole macrocycle in solution.

ASSOCIATED CONTENT

Supporting Information

The Supporting Information is available free of charge on the ACS Publications website at DOI:

Supporting Information. ^{1}H NMR (and ^{19}F NMR) of corroles **1-10**. MS (MALDI/TOF) and HRMS (ESI) spectra of corroles **1-10**. UV-visible spectra of **1-10** in 0.1 M TBAF/CH_2Cl_2. Cyclic voltammograms of compounds **1-10** in CH_2Cl_2 containing 0.1 M $TBAClO_4$. Cyclic voltammograms of compounds **1-10** in DMSO containing 0.1 M $TBAClO_4$. Cyclic voltammograms of compound **7** in CH_2Cl_2 containing 0.1 M $TBAClO_4$ and 0 to 77 equiv of TBACN.

AUTHOR INFORMATION

Corresponding Authors

*E-mail: roberto.paolesse@uniroma2.it. Phone: +39 06 72 59 47 52

*E-mail: claude.gros@u-bourgogne.fr. Phone: +33 (0)3 80 39 61 12.

*E-mail: kkadish@uh.edu. Phone: (+1) 713-743-2740.

ORCID

W. Ryan Osterloh: 0000-0001-9127-2519

Valentin Quesneau: 0000-0002-5996-4811

Nicolas Desbois: 0000-0002-1156-4608

Roberto Paolesse: 0000-0002-2380-1404

Claude P. Gros: 0000-0002-6966-947X

Karl M. Kadish: 0000-0003-4586-6732

Notes

The authors declare no competing financial interest.

ACKNOWLEDGEMENTS

This work was supported by the Robert A. Welch Foundation (K.M.K., Grant E-680). Support was provided by the CNRS (UMR UB-CNRS 6302), the "Université Bourgogne Franche-Comté", the FEDER-FSE Bourgogne 2014/2020 (European Regional Development Fund) and the "Conseil Régional de Bourgogne" through the PARI II CDEA project and the JCE program. V.Q. warmly thanks CRB for PhD grant. The French Research Agency (ANR) is also acknowledged for financial support (CO^3SENS project). The authors wish also to warmly thank Mrs Sandrine Pacquelet for technical assistance.

REFERENCES

1. Erben, C.; Will, S.; Kadish, K. M. In *Metallocorroles: Molecular Structure, Spectroscopy and Electronic States,* Academic Press: 2000; pp 233-300.

2. Ghosh, A.; Steene, E., High-Valent Transition Metal Centers Versus Noninnocent Ligands in Metallocorroles: Insights from Electrochemistry and Implications for High-Valent Heme Protein Intermediates. *J. Inorg. Biochem.* **2002,** *91*, 423-436.

3. Guilard, R.; Barbe, J.-M.; Stern, C.; Kadish, K. M. In *New Developments in Corrole Chemistry: Special Emphasis on Face-to-Face Bismacrocycles*, Elsevier Science: 2003; pp 303-349.

4. Gross, Z.; Gray, H. B., Oxidations Catalyzed by Metallocorroles. *Adv. Synth. Catal.* **2004,** *346*, 165-170.

5. Ali, H.; van Lier, J. E. In *Porphyrins and Phthalocyanines as Photosensitizers and Radiosensitizers*, World Scientific Publishing Co. Pte. Ltd.: 2010; pp 1-119.

6. Aviv-Harel, I.; Gross, Z., Coordination Chemistry of Corroles with Focus on Main Group Elements. *Coord. Chem. Rev.* **2011,** *255*, 717-736.

7. Ghosh, A., Electronic Structure of Corrole Derivatives: Insights from Molecular Structures, Spectroscopy, Electrochemistry, and Quantum Chemical Calculations. *Chem. Rev.* **2017,** *117*, 3798-3881.

8. Fang, Y.; Ou, Z.; Kadish, K. M., Electrochemistry of Corroles in Nonaqueous Media. *Chem. Rev.* **2017,** *117*, 3377-3419.

9. Fremond, L. Catalysis of the Electroreduction of Dioxygen by Cobalt(III) Corrole. Reactivity of Monocorrole, Biscorrole and Porphyrin-Corrole Dyads. 2007.

10. Schechter, A.; Stanevsky, M.; Mahammed, A.; Gross, Z., Four-Electron Oxygen Reduction by Brominated Cobalt Corrole. *Inorg. Chem.* **2012,** *51*, 22-24.

11. Mondal, B.; Sengupta, K.; Rana, A.; Mahammed, A.; Botoshansky, M.; Dey, S. G.; Gross, Z.; Dey, A., Cobalt Corrole Catalyst for Efficient Hydrogen Evolution Reaction from H2O under Ambient Conditions: Reactivity, Spectroscopy, and Density Functional Theory Calculations. *Inorg. Chem.* **2013,** *52*, 3381-3387.

12. Mahammed, A.; Mondal, B.; Rana, A.; Dey, A.; Gross, Z., The Cobalt Corrole Catalyzed Hydrogen Evolution Reaction: Surprising Electronic Effects and Characterization of Key Reaction Intermediates. *Chem. Commun.* **2014,** *50*, 2725-2727.

13. Mahammed, A.; Gross, Z., Metallocorroles as Electrocatalysts for the Oxygen Reduction Reaction (ORR). *Isr. J. Chem.* **2016,** *56*, 756-762.

14. Zhang, W.; Lai, W.; Cao, R., Energy-Related Small Molecule Activation Reactions: Oxygen Reduction and Hydrogen and Oxygen Evolution Reactions Catalyzed by Porphyrin- and Corrole-Based Systems. *Chem. Rev.* **2017,** *117*, 3717-3797.

15. Friedman, A.; Landau, L.; Gonen, S.; Gross, Z.; Elbaz, L., Efficient Bio-Inspired Oxygen Reduction Electrocatalysis with Electropolymerized Cobalt Corroles. *ACS Catal.* **2018,** *8*, 5024-5031.

16. Sinha, W.; Mizrahi, A.; Mahammed, A.; Tumanskii, B.; Gross, Z., Reactive Intermediates Involved in Cobalt Corrole Catalyzed Water Oxidation (and Oxygen Reduction). *Inorg. Chem.* **2018,** *57*, 478-485.

17. Rovira, C.; Kunc, K.; Hutter, J.; Parrinello, M., Structural and Electronic Properties of Co-corrole, Co-corrin, and Co-porphyrin. *Inorg. Chem.* **2001,** *40*, 11-17.

18. Ganguly, S.; Renz, D.; Giles, L. J.; Gagnon, K. J.; McCormick, L. J.; Conradie, J.; Sarangi, R.; Ghosh, A., Cobalt- and Rhodium-Corrole-Triphenylphosphine Complexes Revisited: The Question of a Noninnocent Corrole. *Inorg. Chem.* **2017,** *56*, 14788-14800.

19. Ganguly, S.; Conradie, J.; Bendix, J.; Gagnon, K. J.; McCormick, L. J.; Ghosh, A., Electronic Structure of Cobalt-Corrole-Pyridine Complexes: Noninnocent Five-Coordinate Co(II) Corrole-Radical States. *J. Phys. Chem. A* **2017,** *121*, 9589-9598.

20. Kadish, K. M.; Shao, J.; Ou, Z.; Gros, C. P.; Bolze, F.; Barbe, J.-M.; Guilard, R., Alkyl- and Aryl-Substituted Corroles. 4. Solvent Effects on the Electrochemical and Spectral Properties of Cobalt Corroles. *Inorg. Chem.* **2003,** *42*, 4062-4070.

21. Kadish, K. M.; Fremond, L.; Ou, Z.; Shao, J.; Shi, C.; Anson, F. C.; Burdet, F.; Gros, C. P.; Barbe, J.-M.; Guilard, R., Cobalt(III) Corroles as Electrocatalysts for the Reduction of Dioxygen: Reactivity of a Monocorrole, Biscorroles, and Porphyrin-Corrole Dyads. *J. Am. Chem. Soc.* **2005,** *127*, 5625-5631.

22. Kadish, K. M.; Shen, J.; Fremond, L.; Chen, P.; El Ojaimi, M.; Chkounda, M.; Gros, C. P.; Barbe, J.-M.; Ohkubo, K.; Fukuzumi, S.; Guilard, R., Clarification of the Oxidation State of Cobalt Corroles in Heterogeneous and Homogeneous Catalytic Reduction of Dioxygen. *Inorg. Chem.* **2008,** *47*, 6726-6737.

23. Chen, P.; El Ojaimi, M.; Gros, C. P.; Barbe, J.-M.; Guilard, R.; Shen, J.; Kadish, K. M., Electrochemistry and Spectroelectrochemistry of Bismanganese Biscorroles Dyads. *J. Porphyrins Phthalocyanines* **2011,** *15*, 188-196.

24. Chen, P.; El Ojaimi, M.; Gros, C. P.; Richard, P.; Barbe, J.-M.; Guilard, R.; Shen, J.; Kadish, K. M., Electrochemistry and Spectroelectrochemistry of Bismanganese Porphyrin-Corrole Dyads. *Inorg. Chem.* **2011,** *50*, 3479-3489.

25. Gros, C. P.; Brisach, F.; Meristoudi, A.; Espinosa, E.; Guilard, R.; Harvey, P. D., Modulation of the Singlet-Singlet Through-Space Energy Transfer Rates in Cofacial Bisporphyrin and Porphyrin-Corrole Dyads. *Inorg. Chem.* **2007,** *46*, 125-135.

26. Shen, J.; El Ojaimi, M.; Chkounda, M.; Gros, C. P.; Barbe, J.-M.; Shao, J.; Guilard, R.; Kadish, K. M., Solvent, Anion, and Structural Effects on the Redox Potentials and UV-visible Spectral Properties of Mononuclear Manganese Corroles. *Inorg. Chem.* **2008,** *47*, 7717-7727.

27. Licoccia, S.; Paolesse, R., Metal Complexes of Corroles and Other Corrinoids. *Struct. Bonding (Berlin)* **1995,** *84*, 71-133.

28. Nardis, S.; Monti, D.; Paolesse, R., Novel aspects of corrole chemistry. *Mini-Rev. Org. Chem.* **2005,** *2*, 355-374.

29. Paolesse, R., Corrole: the Little Big Porphyrinoid. *Synlett* **2008**, 2215-2230.

30. Paolesse, R. In *Syntheses of Corroles*, Academic Press: 2000; pp 201-232.

31. Jiang, X.; Naitana, M. L.; Desbois, N.; Quesneau, V.; Brandes, S.; Rousselin, Y.; Shan, W.; Osterloh, W. R.; Blondeau-Patissier, V.; Gros, C. P.; Kadish, K. M., Electrochemistry of Bis(pyridine)cobalt (Nitrophenyl)corroles in Nonaqueous Media. *Inorg. Chem.* **2018,** *57*, 1226-1241.

32. Quesneau, V.; Shan, W.; Desbois, N.; Brandes, S.; Rousselin, Y.; Vanotti, M.; Blondeau-Patissier, V.; Naitana, M.; Fleurat-Lessard, P.; Van Caemelbecke, E.; Kadish, K. M.; Gros, C. P., Cobalt Corroles with Bis-Ammonia or Mono-DMSO Axial Ligands. Electrochemical, Spectroscopic Characterizations and Ligand Binding Properties. *Eur. J. Inorg. Chem.* **2018,** *2018*, 4265-4277.

33. Jiang, X.; Shan, W.; Desbois, N.; Quesneau, V.; Brandes, S.; Van Caemelbecke, E.; Osterloh, W. R.; Blondeau-Patissier, V.; Gros, C. P.; Kadish, K. M., Mono-DMSO ligated cobalt

nitrophenylcorroles: electrochemical and spectral characterization. *New J. Chem.* **2018,** *42*, 8220-8229.

34. Kadish, K. M.; Shao, J.; Ou, Z.; Fremond, L.; Zhan, R.; Burdet, F.; Barbe, J.-M.; Gros, C. P.; Guilard, R., Electrochemistry, Spectroelectrochemistry, Chloride Binding, and O_2 Catalytic Reactions of Free-Base Porphyrin-Cobalt Corrole Dyads. *Inorg. Chem.* **2005,** *44*, 6744-6754.

35. Gross, Z.; Galili, N.; Simkhovich, L.; Saltsman, I.; Botoshansky, M.; Blaser, D.; Boese, R.; Goldberg, I., Solvent-Free Condensation of Pyrrole and Pentafluorobenzaldehyde: A Novel Synthetic Pathway to Corrole and Oligopyrromethenes. *Org. Lett.* **1999,** *1*, 599.

36. Koszarna, B.; Gryko, D. T., Efficient Synthesis of *meso*-Substituted Corroles in a H_2O-MeOH Mixture. *J. Org. Chem.* **2006,** *71*, 3707-3717.

37. Alemayehu, A.; Ghosh, A. In *Geometric and electronic structure of platinum corroles: Excited-state signatures of ligand noninnocence [abstract]*, 248th ACS National Meeting & Exposition; 2014 Aug. 10-14, San Francisco, CA, San Francisco, CA, 2014. Abstract nr INORG-495.

38. Ganguly, S.; Ghosh, A., Seven Clues to Ligand Noninnocence: The Metallocorrole Paradigm. *Acc. Chem. Res.* **2019,** *52*, 2003-2014.

39. Ganguly, S.; Giles, L. J.; Thomas, K. E.; Sarangi, R.; Ghosh, A., Ligand Noninnocence in Iron Corroles: Insights from Optical and X-ray Absorption Spectroscopies and Electrochemical Redox Potentials. *Chem. Eur. J.* **2017,** *23*, 15098-15106.

40. Ganguly, S.; McCormick, L. J.; Conradie, J.; Gagnon, K. J.; Sarangi, R.; Ghosh, A., Electronic Structure of Manganese Corroles Revisited: X-ray Structures, Optical and X-ray Absorption Spectroscopies, and Electrochemistry as Probes of Ligand Noninnocence. *Inorg. Chem.* **2018,** *57*, 9656-9669.

41. Norheim, H.-K.; Capar, J.; Einrem, R. F.; Gagnon, K. J.; Beavers, C. M.; Vazquez-Lima, H.; Ghosh, A., Ligand Noninnocence in FeNO Corroles: Insights from β-Octabromocorrole Complexes. *Dalton Trans.* **2016,** *45*, 681-689.

42. Sarangi, R.; Giles, L. J.; Thomas, K. E.; Ghosh, A., Ligand Noninnocence in Silver Corroles: A XANES Investigation. *Eur. J. Inorg. Chem.* **2016,** *2016*, 3225-3227.

43. Thomas, K. E.; Vazquez-Lima, H.; Fang, Y.; Song, Y.; Gagnon, K. J.; Beavers, C. M.; Kadish, K. M.; Ghosh, A., Ligand Noninnocence in Coinage Metal Corroles: A Silver Knife-Edge. *Chem. Eur. J.* **2015,** *21*, 16839-16847.

44. Vazquez-Lima, H.; Norheim, H.-K.; Einrem, R. F.; Ghosh, A., Cryptic Noninnocence: FeNO Corroles in a New Light. *Dalton Trans.* **2015,** *44*, 10146-10151.

45. Sinha, W.; Mizrahi, A.; Mahammed, A.; Tumanskii, B.; Gross, Z., Reactive Intermediates Involved in Cobalt Corrole Catalyzed Water Oxidation (and Oxygen Reduction). *Inorg. Chem.* **2018,** *57*, 478-485.

46. Pomarico, G.; Galloni, P.; Mandoj, F.; Nardis, S.; Stefanelli, M.; Vecchi, A.; Lentini, S.; Cicero, D. O.; Cui, Y.; Zeng, L.; Kadish, K. M.; Paolesse, R., 5,10,15-Triferrocenylcorrole Complexes. *Inorg. Chem.* **2015,** *54*, 10256-10268.

47. Saha, S., Anion-Induced Electron Transfer. *Acc. Chem. Res.* **2018,** *51*, 2225-2236.

48. Guha, S.; Saha, S., Fluoride Ion Sensing by an Anion-π Interaction. *J. Am. Chem. Soc.* **2010,** *132*, 17674-17677.

49. Hammett, L. P., *Physical Organic Chemistry*. Wiley: New York, 1970.

50. Zuman, P., *Substituent effects in organic polarography*. Plenum Press: New York, 1967.

51. Kadish, K. M.; Morrison, M. M., Substituent Effects on the Oxidation-Reduction Reactions of Nickel Para-Substituted Tetraphenylporphyrin in Nonaqueous Media. *Inorg. Chem.* **1976,** *15*, 980-982.

52. Kadish, K. M.; Morrison, M. M., Substituent Effects on the Redox Reactions of Tetraphenylporphyrins. *Bioinorg. Chem.* **1977,** *7*, 107-115.

53. Kadish, K. M.; Van Caemelbecke, E.; Royal, G., 55 - Electrochemistry of Metalloporphyrins in Nonaqueous Media. In *The Porphyrin Handbook*, Kadish, K. M.; Smith, K. M.; Guilard, R., Eds. Academic Press: 2000; Vol. 9, pp 1-97.

54. Walker, F. A.; Beroiz, D.; Kadish, K. M., Electronic Effects in Transition Metal Porphyrins. 2. The Sensitivity of Redox and Ligand Addition Reactions in *para*-Substituted Tetraphenylporphyrin Complexes of Cobalt(II). *J. Am. Chem. Soc.* **1976,** *98*, 3484-3489.

55. Li, B.; Ou, Z.; Meng, D.; Tang, J.; Fang, Y.; Liu, R.; Kadish, K. M., Cobalt Triarylcorroles Containing One, Two or Three Nitro Groups. Effect of NO_2 Substitution on Electrochemical Properties and Catalytic Activity for Reduction of Molecular Oxygen in Acid Media. *J. Inorg. Biochem.* **2014,** *136*, 130-139.

56. Ou, Z.; Lü, A.; Meng, D.; Huang, S.; Fang, Y.; Lu, G.; Kadish, K. M., Molecular Oxygen Reduction Electrocatalyzed by *meso*-Substituted Cobalt Corroles Coated on Edge-Plane Pyrolytic Graphite Electrodes in Acidic Media. *Inorg. Chem.* **2012,** *51*, 8890-8896.

57. Adamian, V. A.; D'Souza, F.; Licoccia, S.; Di Vona, M. L.; Tassoni, E.; Paolesse, R.; Boschi, T.; Kadish, K. M., Synthesis, Characterization, and Electrochemical Behavior of (5,10,15-Tri-X-phenyl-2,3,7,8,12,13,17,18-octamethylcorrolato)cobalt(III) Triphenylphosphine Complexes, Where X = *p*-OCH3, *p*-CH3, *p*-Cl, *m*-Cl, *o*-Cl, *m*-F, or *o*-F. *Inorg. Chem.* **1995,** *34*, 532-540.

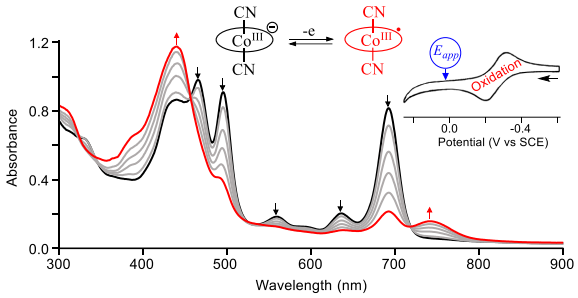

TOC Synopsis. A new series of cobalt A_3-triarylcorroles was synthesized and the compounds examined as to their electrochemical and spectroscopic properties in CH_2Cl_2 or DMSO containing ten different anions added to solution in the form of tetrabutylammonium salts.